THE JOURNAL OF BIOLOGICAL CHEMISTRY VOL. 290, NO. 10, pp. 6086–6105, March 6, 2015

Phosphatidylinositol 3-Kinase Class II α-Isoform PI3K-C2α Is Required for Transforming Growth Factor β-induced Smad Signaling in Endothelial Cells*[S]

Received for publication, July 31, 2014, and in revised form, January 17, 2015 Published, JBC Papers in Press, January 22, 2015, DOI 10.1074/jbc.M114.601484

Sho Aki[‡], Kazuaki Yoshioka[‡], Yasuo Okamoto[‡], Noriko Takuwa[‡§], and Yoh Takuwa[‡1]

From the [‡]Department of Physiology, Kanazawa University School of Medicine, Kanazawa, Ishikawa 920-8640, Japan and the [§]Department of Health and Medical Sciences, Ishikawa Prefectural Nursing University, Kahoku, Ishikawa 929-1210, Japan

Background: TGFβ receptor signals through Smad phosphorylation, which is dependent on endocytosis of TGFβ receptors and the Smad anchor protein SARA localized on endosomes.
Results: Class II PI3K-C2α is necessary for TGFβ receptor endocytosis into SARA-containing endosomes, SARA-Smad complex formation, and Smad phosphorylation.
Conclusion: PI3K-C2α serves endosomal TGFβ receptor signaling.
Significance: PI3K-C2α is a key molecule that is generally engaged in endosomal receptor signaling.

We have recently demonstrated that the PI3K class II-α isoform (PI3K-C2α), which generates phosphatidylinositol 3-phosphate and phosphatidylinositol 3,4-bisphosphates, plays crucial roles in angiogenesis, by analyzing PI3K-C2α knock-out mice. The PI3K-C2α actions are mediated at least in part through its participation in the internalization of VEGF receptor-2 and sphingosine-1-phosphate receptor $S1P_1$ and thereby their signaling on endosomes. TGFβ, which is also an essential angiogenic factor, signals via the serine/threonine kinase receptor complex to induce phosphorylation of Smad2 and Smad3 (Smad2/3). SARA (Smad anchor for receptor activation) protein, which is localized in early endosomes through its FYVE domain, is required for Smad2/3 signaling. In the present study, we showed that PI3K-C2α knockdown nearly completely abolished TGFβ1-induced phosphorylation and nuclear translocation of Smad2/3 in vascular endothelial cells (ECs). PI3K-C2α was necessary for TGFβ-induced increase in phosphatidylinositol 3,4-bisphosphates in the plasma membrane and TGFβ receptor internalization into the SARA-containing early endosomes, but not for phosphatidylinositol 3-phosphate enrichment or localization of SARA in the early endosomes. PI3K-C2α was also required for TGFβ receptor-mediated formation of SARA-Smad2/3 complex. Inhibition of dynamin, which is required for the clathrin-dependent receptor endocytosis, suppressed both TGFβ receptor internalization and Smad2/3 phosphorylation. TGFβ1 stimulated Smad-dependent VEGF-A expression, VEGF receptor-mediated EC migration, and capillary-like tube formation, which were all abolished by either PI3K-C2α knockdown or a dynamin inhibitor. Finally, TGFβ1-induced microvessel formation in Matrigel plugs was greatly attenuated in EC-specific PI3K-C2α-deleted mice. These observations indicate that PI3K-C2α plays the pivotal role in TGFβ receptor endocytosis and thereby Smad2/3 signaling, participating in angiogenic actions of TGFβ.

PI3Ks are a family of enzymes that phosphorylate membrane inositol phospholipids at the 3′ position of the inositol ring and comprise three classes (classes I–III) (1, 2). Class I PI3Ks, which mainly generate phosphatidylinositol 3,4,5-bisphosphates, are activated by receptor tyrosine kinases and G protein-coupled receptors to mediate activation of Akt and Rac, stimulating cell proliferation and migration. In contrast to the well characterized class I PI3Ks, physiological roles of class II PI3Ks, which have three members: PI3K-C2α, PI3K-C2β, and PI3K-C2γ, were not well understood (3–7). We have recently revealed that PI3K-C2α plays a crucial role in angiogenesis and maintenance of the endothelial barrier integrity in an endothelial cell (EC)[2] autonomous manner (8). PI3K-C2α is localized in clathrin-coated pits and endocytic vesicles, early endosomes, and the *trans*-Golgi network (8–11) and is thought to predominantly generate phosphatidylinositol 3-phosphate (PtdIns(3)P) and/or phosphatidylinositol 3,4-bisphosphates ($PtdIns(3,4)P_2$) *in vivo* differently from class I PI3K (3–5, 7, 12–14). Our data showed that PI3K-C2α regulates vesicular trafficking in EC and thereby is indispensable for vesicular transport-mediated delivery of cargos including the endothelial adhesion molecule VE-cadherin and ligand binding-induced endocytosis of the receptor tyrosine kinase VEGF receptor-2 (VEGFR2) and the G protein-

* This work was supported in part by grants-in-aid from the Japanese Ministry of Education, Culture, Sports, Science, and Technology, the Japanese Society for the Promotion of Science, the Ube foundation, the Japan Foundation for Applied Enzymology, and the Life Science Foundation of Japan.
[S] This article contains supplemental Movies S1 and S2.
[1] To whom correspondence should be addressed: Dept. of Physiology, Kanazawa University School of Medicine, 13-1 Takara-machi, Kanazawa, Ishikawa 920-8640 Japan. Tel.: 81-76-265-2165; Fax: 81-76-234-4223; E-mail: ytakuwa@med.kanazawa-u.ac.jp.

[2] The abbreviations used are: EC, endothelial cell; HUVEC, human umbilical vein endothelial cell; HMVEC, human microvascular endothelial cell; C2α, PI3K-C2α; C2β, PI3K-C2β; $C2α^r$, C2α-siRNA-resistant C2α; $kdC2α^r$, kinase-deficient mutant of C2α; PtdIns(3)P, phosphatidylinositol 3-phosphate; $PtdIns(3,4)P_2$, phosphatidylinositol 3,4-bisphosphates; ALK, activin receptor-like kinase; wtALK5, wild-type ALK5; caALK5, constitutively active ALK5 mutant; wt, wild-type SARA; S1P, sphingosine-1-phosphate; ΔSBD-SARA, Smad-binding domain-deleted mutant; SMC, smooth muscle cell; VEGFR, VEGF receptor; MLEC, mouse lung endothelial cell; MASM, mouse aortic smooth muscle; vWF, von Willebrand factor; PLA, proximity ligation assay; p-, phosphorylated.

coupled receptor $S1P_1$ (8, 15, 16). Signaling of VEGFR2 and $S1P_1$ was defective in PI3K-C2α-depleted EC: the receptor endocytosis was inhibited, and the signaling on endosomes, particularly Rho GTPase activation, was impaired. These defects result in impaired migration, proliferation, and intercellular junction formation in EC. It is unknown whether and how PI3K-C2α regulates signaling of other angiogenic receptors. In addition to our studies, a general regulatory role for PI3K-C2α in endocytosis through the generation of PtdIns(3,4)P_2 in the plasma membrane was recently reported (14).

TGFβ is involved in the regulation of migration and proliferation of EC, production of basement membrane, and differentiation and recruitment of mural cells, thus being essential for normal vascular formation (17–20). TGFβ signals through type I and type II TGFβ receptors, which are both serine/threonine transmembrane kinases (21–23). TGFβ binds to type II receptor, which phosphorylates and activates type I receptors, activin receptor-like kinase (ALK) 1, and ALK5. ALK1 and ALK5 in turn phosphorylate the receptor-regulated Smads, Smad1 and Smad5 (Smad1/5) and Smad2 and Smad3 (Smad2/3), respectively. Phosphorylated receptor-regulated Smads form complexes with the common mediator Smad4 and the Smad complexes translocate into the nucleus to regulate gene transcription. It was proposed that TGFβ signaling pathways via ALK1 and ALK5 in EC may play a balancing role for controlling proliferation and migration of EC during angiogenesis (24, 25). Of the two TGFβ signaling pathways, EC-specific gene ablation of either ALK5 or Smad2/3 resulted in the similar vascular abnormalities, indicating a pivotal role of endothelial ALK5-Smad2/3 pathway in the angiogenic effect of TGFβ (19, 20, 26, 27). SARA (Smad anchor for receptor activation) protein contains the binding domains for both Smad2/3 and the TGFβ receptor complex and is localized in the early endosomes through its FYVE domain, which specifically recognizes and binds to PtdIns(3)P (28). Previous studies (28–31) demonstrated that upon TGFβ stimulation, the TGFβ receptor complex undergoes clathrin-dependent endocytosis into the early endosomes containing SARA and that the proper localization of SARA in the early endosomes and the TGFβ receptor internalization into the SARA-containing endosomes are the events necessary for TGFβ-induced phosphorylation of Smad2/3 and the following nuclear translocation of the Smad complexes. It is likely that PI3Ks are involved in TGFβ receptor internalization, the endosomal localization of SARA, and thus TGFβ signaling. However, it is unknown which isoform of PI3K is engaged in the processes of TGFβ signaling.

In the present study, we studied a role for PI3K-C2α in TGFβ-induced Smad2/3 signaling in EC. We found that TGFβ-induced Smad2/3 phosphorylation, Smad2/3-dependent gene expression, and angiogenic responses were strongly dependent on PI3K-C2α. PI3K-C2α was required for TGFβ receptor internalization but not the endosomal localization of SARA. These observations suggest that PI3K-C2α plays an indispensable role in endosomal TGFβ receptor signaling.

EXPERIMENTAL PROCEDURES

Cells—Human umbilical vein endothelial cells (HUVECs) (Lonza, Basel, Switzerland), the human microvascular endothelial cells (HMVECs), and mouse lung vascular endothelial cells (MLECs) were plated onto type I collagen (Nitta Gelatin, Osaka, Japan)-coated dishes and flasks and allowed to grow under 5% CO_2 at 37 °C in complete endothelial growth medium containing 2% FBS and growth factor supplements (EGM-2 (catalog no. CC3156; Lonza) for HUVECs and EBM-2-MV (catalog no. CC4147; Lonza) for HMVECs and MLECs). HUVECs between passages 4 and 6 were used for all experiments. MLECs and mouse aortic smooth muscle (MASM) cells were isolated from *Pik3c2a*$^{flox/flox}$ mice and used for *in vitro* assays as described previously (8, 32, 33). HEK293T cells, MASM cells, and Caco2 cells were cultured in 10% FBS (Invitrogen Gibco)-supplemented DMEM for HEK293T and Caco2 cells (catalog no. 041-29775; Invitrogen Gibco) and advanced DMEM for MASM cells (catalog no. 12491; Invitrogen Gibco).

Small Interfering RNA, Plasmids, and Transfection—Knockdown of endogenous PI3K isoforms and Smad4 were performed with the siRNAs that were synthesized using a Silencers siRNA construction kit (catalog no. AM1620; Ambion, Austin, TX) according to the manufacturer's instructions. The target sequences were: 5′-AAGGTTGGCACTTACAAGAAT-3′ and 5′-AAGTAAGCCTAAGGTGGATAA-3′ for human PI3K-C2α #1 and #2, respectively; 5′-AAGCCGGAAGCTTCTGG-GTTT-3′ for PI3K-C2β; 5′–GGACAACTGTTTCATA-TAG-3′ for class I PI3K p110α; 5′-AAACTCAACACTGGCT-AATTA-3′ for Vps34; 5′-AATACATTCCAACTGCACA-CCC-3′ for Smad4; and 5′-GGGGGAAATACGACTTAGTG-AGG-3′ for ALK5. HUVECs were transfected by incubating with the siRNAs in the presence of Lipofectamine 2000 (catalog no. 11668-019; Invitrogen) for 48–72 h before the experiments. MASM cells isolated from *Pik3c2a*$^{flox/flox}$ mice were grown to 70% confluency and then infected with the adenovirus encoding Cre recombinase (Ad-Cre) in the absence of serum. Adenovirus encoding LacZ (Ad-LacZ) was used as control. After 1 h of adenovirus infection, the growth medium containing 10% FBS was added, and the cells were allowed to recover for the next 48 h. The expression vector for GFP-PI3K-C2α was described previously (8). The expression vectors for the PI3K-C2α-specific siRNA-resistant form of PI3K-C2α (C2α^r) and the kinase-deficient mutant (D1268A) of GFP-PI3K-C2α (GFP-kdPI3K-C2α) were generated using a standard PCR-based method (34). In C2α^r, the codons AAG-GTT-GGC-ACT-TAC for the amino acids Lys^{728}-Val^{729}-Gly^{730}-Thr^{731}-Tyr^{732} were replaced by the nucleotides AAA-GTC-GGT-ACC-TAT, which encodes the same amino acids. The changes in these nucleotides rendered C2α^r resistant to the PI3K-C2α-specific siRNA. The expression vectors for FLAG-tagged wild-type SARA (wtSARA), FLAG-tagged Smad-binding domain (the amino acids 665–704)-deleted SARA mutant (ΔSBD-SARA), FLAG-tagged wild-type ALK5 (wtALK5), FLAG-tagged constitutively activated mutant (T202D) of ALK5 (caALK5), and GFP-PH^{TAPP1} were purchased from Addgene (Cambridge, MA). The expression vector for GFP-$FYVE^{SARA}$ was provided by Dr. S. Itoh (Showa Pharmaceutical University) (26). The expression vectors for FLAG-tagged Smad2 and FLAG-tagged Smad3 were provided by Dr. K. Miyazono (University of Tokyo) (35).

Immunoblotting and Immunoprecipitation Analysis—At 48 h after siRNA transfection, the cells were serum-starved

with M199 (Invitrogen Gibco) containing 0.5% fatty acid-free BSA (catalog no. A6003; Sigma-Aldrich) for 4 h and then stimulated with 5 ng/ml TGFβ1 (catalog no. 240-B; R&D Systems, Minneapolis, MN). The cells were washed in PBS and lysed in the cell lysis buffer (20 mM Tris-HCl, pH 7.2, 150 mM NaCl, 1 mM $CaCl_2$, 0.5% Triton X-100, 100 mM NaF, 1 mM Na_3VO_4) supplemented with Complete Protease inhibitor mixture (Roche Applied Science) by scraping, followed by centrifugation for 15 min at 16,000 × *g* at 4 °C. The resultant supernatants were taken, electrophoresed on 8% SDS-PAGE, and transferred onto PVDF membrane (Millipore, Billerica, MA). The membranes were blocked in PBS containing 5% BSA and incubated with respective antibodies overnight. The antibodies used are PI3K-C2α (catalog no. 611046; BD Biosciences, San Jose, CA), PI3K-C2β (catalog no. 611342; BD Biosciences), p110α (catalog no. 4249; Cell Signaling, Danvers, MA), Vps34 (catalog no. 4263; Cell Signaling), total Smad2/3 (catalog no. 610842; BD Biosciences), phosphorylated Smad2 (p-Smad2) (catalog no. 3101; Cell Signaling), phosphorylated Smad3 (p-Smad3) (catalog no. 9520; Cell Signaling), total ERK1/2 (catalog no. 9102; Cell Signaling), phosphorylated ERK1/2 (catalog no. 4370; Cell Signaling), total Smad4 (catalog no. 9515; Cell Signaling); SARA (catalog no. sc-9135; Santa Cruz, Dallas, TX), phosphoserine (catalog no. 618100; Invitrogen), and β-actin (catalog no. A1978; Sigma-Aldrich). The membranes were incubated with alkaline phosphatase-conjugated secondary antibodies (anti-mouse IgG antibody, catalog no. 7056; anti-rabbit IgG antibody, catalog no. 7054) (Cell Signaling) and visualized by color reaction using 5-bromo-4-chloro-3-indolyl-phosphate/nitro blue tetrazolium (Wako, Osaka, Japan). The band intensities were determined using Image Gauge (Fuji Film, Tokyo, Japan). The values were normalized for the value of β-actin as a loading control and expressed as multiples over the normalized values of untreated controls.

For immunoprecipitation assay, HEK293T cells were co-transfected with the expression vectors for FLAG-Smad3, either FLAG-SARA or FLAG-ΔSBD-SARA, and either FLAG-wtALK5 or FLAG-constitutively activated ALK5 (caALK5) and 72 h later were lysed in IP buffer (50 mM Tris-HCl, pH 7.5, 150 mM NaCl, 1% Nonidet P-40, 0.5% deoxycholate, 0.1% SDS) supplemented with Complete Protease inhibitor cocktails. The lysates were incubated with anti-SARA antibody for 1 h at 4 °C with rocking, followed by the incubation with protein G-agarose beads (catalog no. 1-719-416; Roche) for 1 h at 4 °C. After the beads were washed five times, they were mixed with 2× Laemmli's SDS sample buffer and boiled. The resultant samples were analyzed with immunoblotting using respective antibodies.

Immunohistochemistry and Immunofluorescence Staining—HUVECs were plated onto type I collagen-coated glass bottom dishes (MatTek Corporation, Ashland, MA) and allowed to adhere to dishes in EGM-2 growth medium overnight. The cells were rinsed with prewarmed PBS once and fixed in prewarmed 4% fresh paraformaldehyde in PBS for 10 min, washed with PBS, and then permeabilized in 0.2% Triton X-100 in PBS for 15 min when necessary. After the cells were incubated with 5% normal goat serum for 60 min to inhibit nonspecific protein binding, the cells were incubated with rabbit polyclonal anti-p-Smad2 antibody (catalog no. AB3849; Millipore), mouse monoclonal anti-Smad2/3 antibody (catalog no. 610842; BD Biosciences), rabbit polyclonal anti-SARA antibody, or mouse monoclonal anti-EEA1 antibody (catalog no. 610456; BD Biosciences) for 2 h at room temperature or overnight at 4 °C. The cells were incubated for 60 min at room temperature with Alexa Fluor 488-conjugated goat anti-mouse (catalog no. A31620; Molecular Probes), Alexa Fluor 488-conjugated goat anti-rabbit (catalog no. A11034), Alexa Fluor 594-conjugated goat anti-mouse (catalog no. A31624), Alexa Fluor 594-conjugated goat anti-rabbit (catalog no. A31620), and secondary antibodies diluted at 1:1000 in PBS. Where appropriate, the cells were counterstained with DAPI (catalog no. D1306; Molecular Probes) for 5 min. The cells were mounted on Fluoromount (catalog no. K024; Diagnostic BioSystems, Pleasanton, CA) and observed under a custom confocal microscope unit as described in detail previously (8). For immunohistochemistry of the sections of Matrigel plugs, the sections of paraformaldehyde-fixed, paraffin-embedded Matrigel plug were deparaffinized and processed in heat-induced target retrieval to unmask the antigen using with target retrieval solution (Dako, Carpinteria, CA) (30). The sections were incubated with Dako blocking solution (catalog no. X0909; Dako) for 10 min to inhibit nonspecific protein binding. After blocking, the sections were stained with rabbit polyclonal anti-von Willebrand factor (vWF) (catalog no. A0082; Dako) for 60 min at room temperature. The sections were incubated with the secondary antibody of an EnVision kit (catalog no. K4002; Dako) for 60 min, and the color reaction was developed. Where appropriate, the sections were counterstained with hematoxylin. The sections were examined using a BX41 inverted microscope (Olympus, Tokyo, Japan), and vWF-positive microvessel numbers were determined with ImageJ software.

Proximity Ligation Assay (PLA) Staining—The cells were fixed in prewarmed 4% fresh paraformaldehyde in PBS for 10 min and permeabilized in 0.2% Triton X-100 in PBS for 15 min when necessary. After the cells were incubated with rabbit polyclonal anti-ALK5 antibody (catalog no. sc-398; Santa Cruz), mouse monoclonal anti-Smad2/3 antibody, and mouse monoclonal anti-SARA (catalog no. sc-133071; Santa Cruz) antibody overnight at 4 °C, *in situ* protein interactions were detected using the Duolink proximity ligation assay kit according to the manufacturer's instructions (Olink Bioscience, Uppsala, Sweden). The cells were stained with anti-EEA1-Alexa Fluor 594 (M176 A59; MBL, Nagoya, Japan).

RNA Isolation and Quantitative PCR Analysis—Total RNA in HUVECs was isolated using TRIzol reagent (Invitrogen). One μg of total RNA was reverse-transcribed into the first strand cDNA using QuantiTect RT Kit (catalog no. 205311; Qiagen). Quantitative real time PCRs were performed using FAM-conjugated TaqMan inventoried assay from Applied Biosystems for human PI3K-C2α (Hs0090461_m1) and human VEGF-A (Hs00900055_m1). 18 S rRNA (Hs99999901_s1) probe was used as an internal control. The mRNA expression levels were normalized for the expression of 18 S rRNA mRNA, and the results were expressed as multiples over control values. Comparative quantitative analysis was performed using the GeneAmp 7300 system (Applied Biosystems, Foster City, CA) based on the ΔΔCt method.

Wound Healing/Scratch and Tube Formation Assay—For wound healing/scratch assay (32), confluent HUVEC monolayers were scratched with a standard 20-μl pipette tip and incubated in M199 containing 1% FBS in the presence of recombinant human VEGF-A (50 ng/ml) (catalog no. 100-20; PeproTech, Rocky Hill, NJ), TGFβ1 (5 ng/ml), dynasore (80 μM) (catalog no. D7693; Sigma-Aldrich), ALK5 inhibitor II (2-(3-(6-methylpyridin-2-yl)-1-*H*-pyrazol-4-yl)-1,5-naphthyridine) (5 μM) (catalog no. 616452; Merck-CalbioChem), and VEGFR2 inhibitor SU1498 (10 μM) (catalog no. 572888; Merck-Calbiochem) for 8 h. The microphotographs were taken at 0 and 8 h, and the wound width was determined with ImageJ software. For tube formation assays, siRNA-transfected HUVECs (2.0×10^4 cells) in M199 containing 1% FBS were seeded onto 200 μl of growth factor-reduced Matrigel (BD Biosciences) in a 24-well plate in the absence and presence of VEGF-A (50 ng/ml), TGFβ1 (5 ng/ml), dynasore (80 μM), ALK5 inhibitor (5 μM), and VEGFR2 inhibitor (10 μM) and were incubated for 12 h. Tube formation was quantified by measuring cumulative tube length in five random microscopic fields/well using ImageJ software under a BIOREVO microscope (Keyence, Osaka, Japan).

Matrigel Plug in Vivo Angiogenesis Assay—All of the mice used in this study were bred and maintained at the Institute for Experimental Animals, Advanced Science Research Center, Kanazawa University under specific pathogen-free conditions. All procedures were conducted in accordance with the Fundamental Guidelines for Proper Conduct of Animal Experiment and Related Activities in Academic Research Institutions under the jurisdiction of the Ministry of Education, Culture, Sports, Science and Technology of Japan and approved by the Committee on Animal Experimentation of Kanazawa University. *Pik3c2a*$^{\Delta EC}$ (C2α$^{\Delta EC}$) (*Pik3c2a*$^{flox/flox}$; *Cdh5*(PAC)-*CreER*^{T2}) and *Pik3c2a*$^{\Delta SMC}$ (C2α$^{\Delta SMC}$) (*Pik3c2a*$^{flox/flox}$; *SM22a-Cre*) mice were described previously (8). Cre-negative littermates were used as controls. To verify the efficiency of Cre recombination, Cre mice were mated with mice from the Cre reporter transgenic line *ROSA26*-LacZ (B6.129S4-*Gt(ROSA)26Sor*tm1Sor/J, Jackson Lab). All mice had a C57BL/6J genetic background. For *Pik3c2a* gene inactivation in adult mice, tamoxifen (10 mg/ml corn oil) (catalog no. T5648; Sigma-Aldrich) was administered seven times by intraperitoneal injection of 100 μl of tamoxifen solution. For Matrigel plug assay (32, 36), recombinant VEGF-A (200 ng/ml), FGF2 (400 ng/ml) (catalog no. AF-100-18B; PeproTech), and heparin (100 mg/ml) (Sigma-Aldrich) were mixed with growth factor-reduced Matrigel. The Matrigel solutions (300 μl each) were injected subcutaneously into the groin area close to the dorsal midline (most angiogenic portion) of anesthetized mice. Matrigel plugs were harvested on day 10 and fixed overnight in 4% paraformaldehyde for paraffin embedding and the following immunohistochemistry.

VEGF-A ELISA Assay—Human VEGF-A protein levels in the conditioned medium of HUVEC cultures were determined using human VEGF-A ELISA immunoassay (catalog no. DVE00; R&D Systems, Minneapolis, MN) according to the manufacturer's protocol. Optical density was measured at 450 nm using a 540-nm correction with a Multiskan GO (Thermo Fisher Scientific, Walyham, MA).

Statistical Analysis—The data are presented as means ± S.E. and expressed as the percentages or multiples relative to the values in control cells. Statistical significance was analyzed using Prism 5 software (GraphPad Software Inc., San Diego, CA). Statistical significance was analyzed either by one-way or two-way analysis of variance followed by Bonferroni test as appropriate. Results with $p < 0.05$ were considered statistically significant.

RESULTS

TGFβ1-induced Phosphorylation and Nuclear Translocation of Smad2/3 Are Dependent on Class II PI3K-C2α—We studied roles of PI3K isoforms in TGFβ1-induced Smad2/3 stimulation in vascular EC. HUVECs were transfected with either of the specific siRNAs against class I PI3K p110α, class II PI3K-C2α and PI3K-C2β, and class III Vps34, or scrambled siRNA (sc-siRNA) as control. Each siRNA effectively inhibited the expression of respective PI3K proteins but not other PI3K isoform proteins (Fig. 1, *A* and *B*). In sc-siRNA-transfected control HUVECs, TGFβ1 induced a gradual increase in Smad3 phosphorylation, which reached the plateau level of an 8-fold increase over the basal at 30 min (Fig. 1*B*). Transfection of PI3K-C2α-siRNAs (C2α-siRNAs #1 and #2) markedly inhibited TGFβ1-induced stimulation of Smad3 phosphorylation throughout the observation time period. TGFβ1 also induced Smad2 phosphorylation, which was greatly suppressed by PI3K-C2α knockdown (Fig. 1*C*). In contrast, knockdown of either p110α, PI3K-C2β, or Vps34 failed to inhibit TGFβ1-induced phosphorylation of Smad2/3. TGFβ1 did not stimulate phosphorylation of Smad1, Smad5, or Smad8 (Smad1/5/8) in HUVECs (Fig. 1*D*). In contrast, BMP9 induced phosphorylation of Smad1/5/8 (Fig. 1*E*) but not Smad2/3 (data not shown). Differently from the case of TGFβ1, PI3K-C2α knockdown did not suppress BMP9-induced Smad1/5/8 phosphorylation. In addition, PI3K-C2α knockdown did not alter TGFβ1-induced activation of the noncanonical pathway ERK, which is known to be independent of Smad2/3 (37), in HUVECs. Similar to HUVECs, TGFβ1 stimulated phosphorylation of Smad2/3 in HMVECs and MLECs in a PI3K-C2α-dependent manner (Fig. 2, *A* and *B*). TGFβ1 also stimulated phosphorylation of Smad1/5/8 in HMVECs, which was also dependent on PI3K-C2α (Fig. 2*A*). Unlike vascular endothelial cells, deletion of PI3K-C2α in MASM cells and human colonic epithelial carcinoma Caco2 cells did not inhibit TGFβ1-induced phosphorylation of Smad2/3 (Fig. 2, *C* and *D*). Thus, PI3K-C2α was necessary for TGFβ-induced Smad2/3 phosphorylation in vascular EC but not in vascular smooth muscle.

Stimulation with TGFβ1 induced robust nuclear translocation of Smad2/3 in sc-siRNA-transfected HUVECs as evaluated with anti-Smad2/3 immunofluorescent staining (Fig. 3*A*). We also observed that TGFβ1 stimulated nuclear accumulation of p-Smad2, which was also markedly suppressed by PI3K-C2α knockdown (Fig. 3*B*). In C2α-siRNA-transfected HUVECs, the exogenous expression of the C2α-siRNA-resistant form of PI3K-C2α (C2α^r) but not wild-type PI3K-C2α (wtC2α) restored TGFβ-induced Smad activation (Fig. 3, *C* and *D*). In sc-siRNA-transfected HUVECs, the overexpression of wild-type PI3K-C2α by itself did not change TGFβ-induced Smad translocation into the nucleus. Moreover, we determined the effect of the expression of the kinase-deficient mutant of C2α^r (kdC2α^r) on Smad2/3

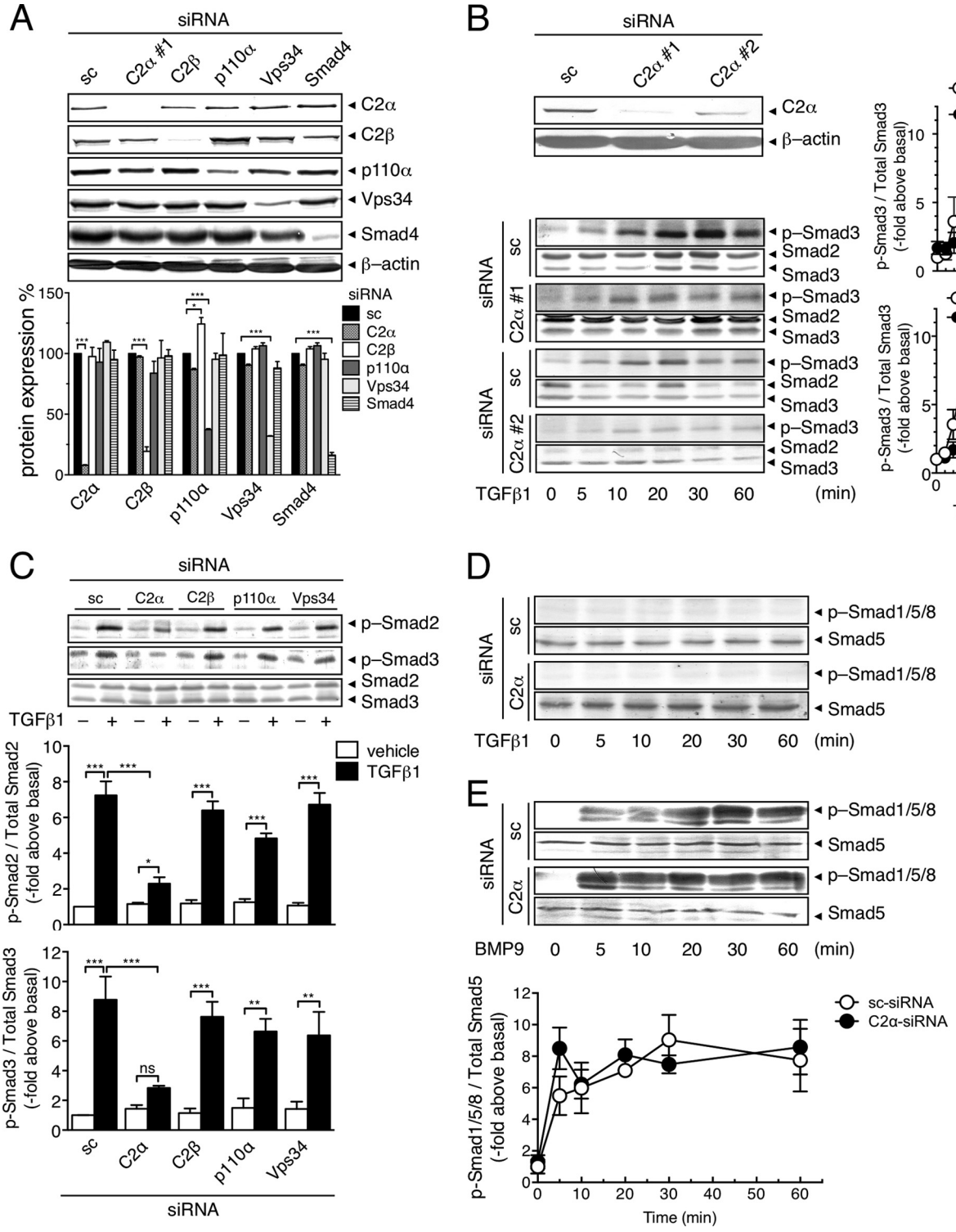

FIGURE 1. **PI3K-C2α is required for TGFβ1-induced Smad2/3 phosphorylation in EC.** *A*, siRNA-mediated knockdown of PI3K isoforms. HUVECs were transfected with PI3K-C2α#1 (C2α#1)-, PI3K-C2β (C2β)-, p110α-, Vps34-, and Smad4-specific siRNA or scrambled (sc)-siRNA, and the expression of the PI3K proteins, Smad4, and β-actin as a loading control were analyzed with immunoblotting. *Upper panel*, representative blots. *Lower panel*, quantified data. *B*, time-dependent phosphorylation of Smad3 in response to TGFβ1 in C2α#1, C2α#2, or sc-siRNA transfected HUVECs. Serum-starved cells were stimulated with TGFβ1 (5 ng/ml) for the indicated time periods. The cell lysates were subjected to immunoblot analysis for p-Smad3 and total Smad2 and Smad3. *Upper left panel*, effects of siRNA-mediated knockdown of PI3K-C2α. *Lower left panel*, representative blots of Smads. *Right panel*, quantified data. *C*, effects of knockdown of PI3K isoforms on TGFβ1-induced Smad2 and Smad3 phosphorylation. HUVECs that had been transfected with either of C2α#1-, C2β-, p110α-, and Vps34-specific siRNAs or sc-siRNA were stimulated with TGFβ1 (5 ng/ml) for 30 min, followed by the immunoblot analysis for p-Smad2, p-Smad3, and total Smad2 and Smad3. *Upper panel*, representative blots. *Lower panel*, quantified data. *D*, time-dependent phosphorylation of Smad1/5/8 in response to TGFβ1 in HUVECs. The cells were treated as in *B*. The cell lysates were subjected to immunoblot analysis for p-Smad1/5/8 and total Smad5. *E*, time-dependent phosphorylation of Smad1/5/8 in response to BMP9 in HUVECs. Serum-starved cells were stimulated with BMP9 (10 ng/ml) for the indicated time periods. The cell lysates were subject to immunoblot analysis for p-Smad1/5/8 and total Smad5. In *A–E*, the data are means ± S.E. of three or four determinations ($n = 3$ or 4.). In all figures, the *asterisks* indicate statistical significance between the indicated groups at the levels of $p < 0.05$ (*), $p < 0.01$ (**), and $p < 0.001$ (***). *ns*, statistically not significant.

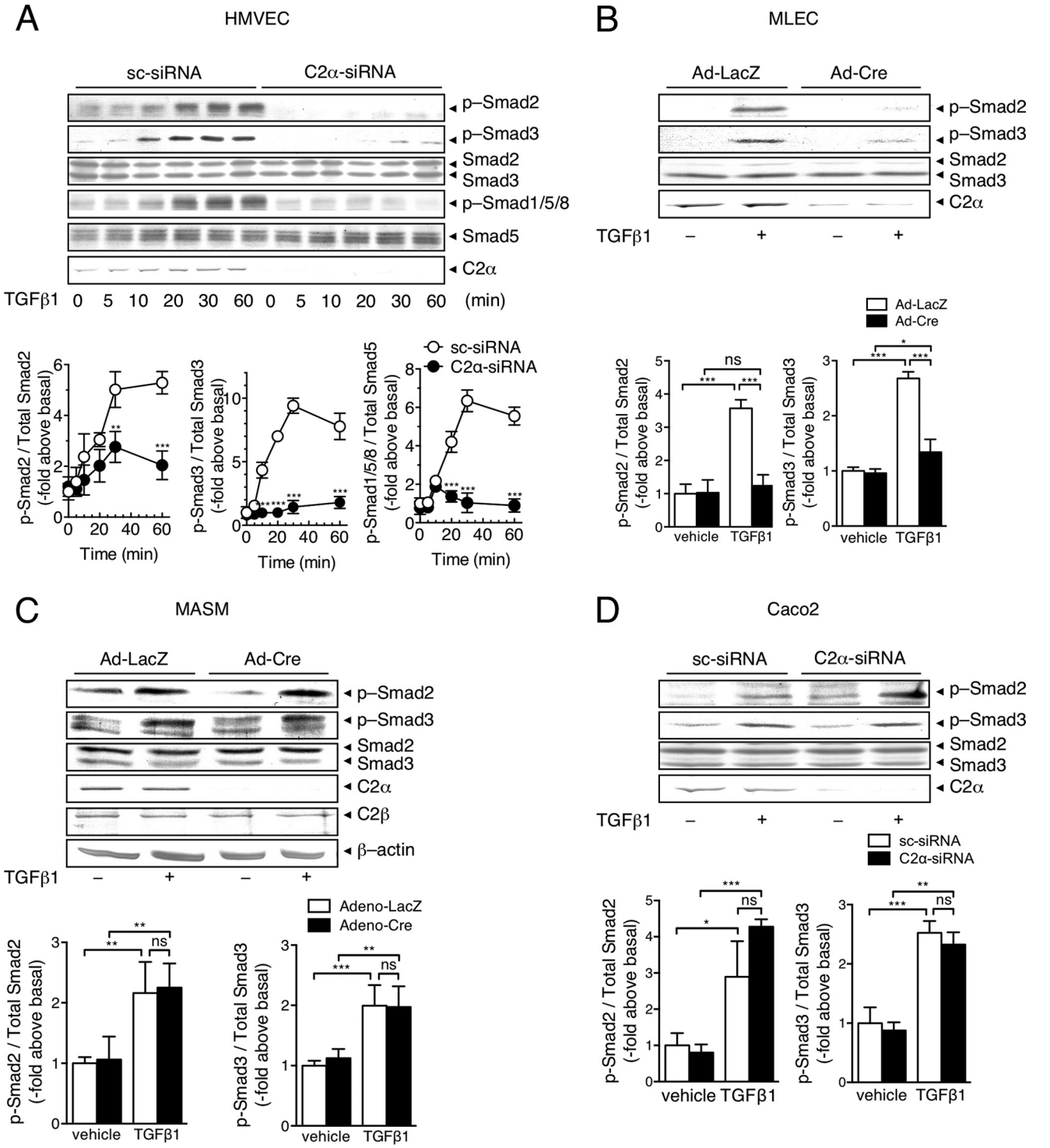

FIGURE 2. **PI3K-C2α is required for TGFβ-induced Smad2/3 phosphorylation in EC but not smooth muscle cells or epithelial cells.** *A*, TGFβ1-induced time-dependent phosphorylation of Smad2/3 and Smad1/5/8 in HMVECs. Serum-starved cells were stimulated with TGFβ1 (5 ng/ml) for the indicated time periods. The cell lysates were subjected to immunoblot analysis for p-Smad1/5/8 and p-Smad2/3. *B*, effects of Cre-mediated deletion of C2α on TGFβ1-induced Smad3 phosphorylation in MLECs. The cells were infected with adenoviruses encoding LacZ (Ad-LacZ) or Cre recombinase (Ad-Cre), stimulated as in *A*, and analyzed for p-Smad3. *C*, effects of Cre-mediated deletion of C2α on TGFβ1-induced Smad3 phosphorylation in MASM cells. The cells were treated and analyzed as in *A*. *D*, effects of knockdown of PI3K isoforms on TGFβ1-induced phosphorylation of Smad2/3. Caco2 were treated and analyzed as in *A*. In *A–D*, *upper panels* indicate representative blots, and *lower panels* indicate quantified data ($n = 3–5$). The data are expressed as multiples relative to the values in TGFβ1-nonstimulated sc-siRNA transfected cells or Ad-Cre-transfected cells.

nuclear translocation. In sc-siRNA-transfected control HUVECs, the expression of kdC2α^r inhibited TGFβ1-induced Smad2/3 nuclear accumulation, differently from wtC2α^r expression (Fig. 3*D*). In C2α-siRNA-transfected HUVECs, the expression of kdC2α^r did not restore TGFβ1-induced Smad2/3 nuclear accumulation, differently from wtC2α^r. These observations together suggest that PI3K-C2α fulfills an indispensable role for TGFβ1-induced Smad2/3 activation through its kinase activity in EC.

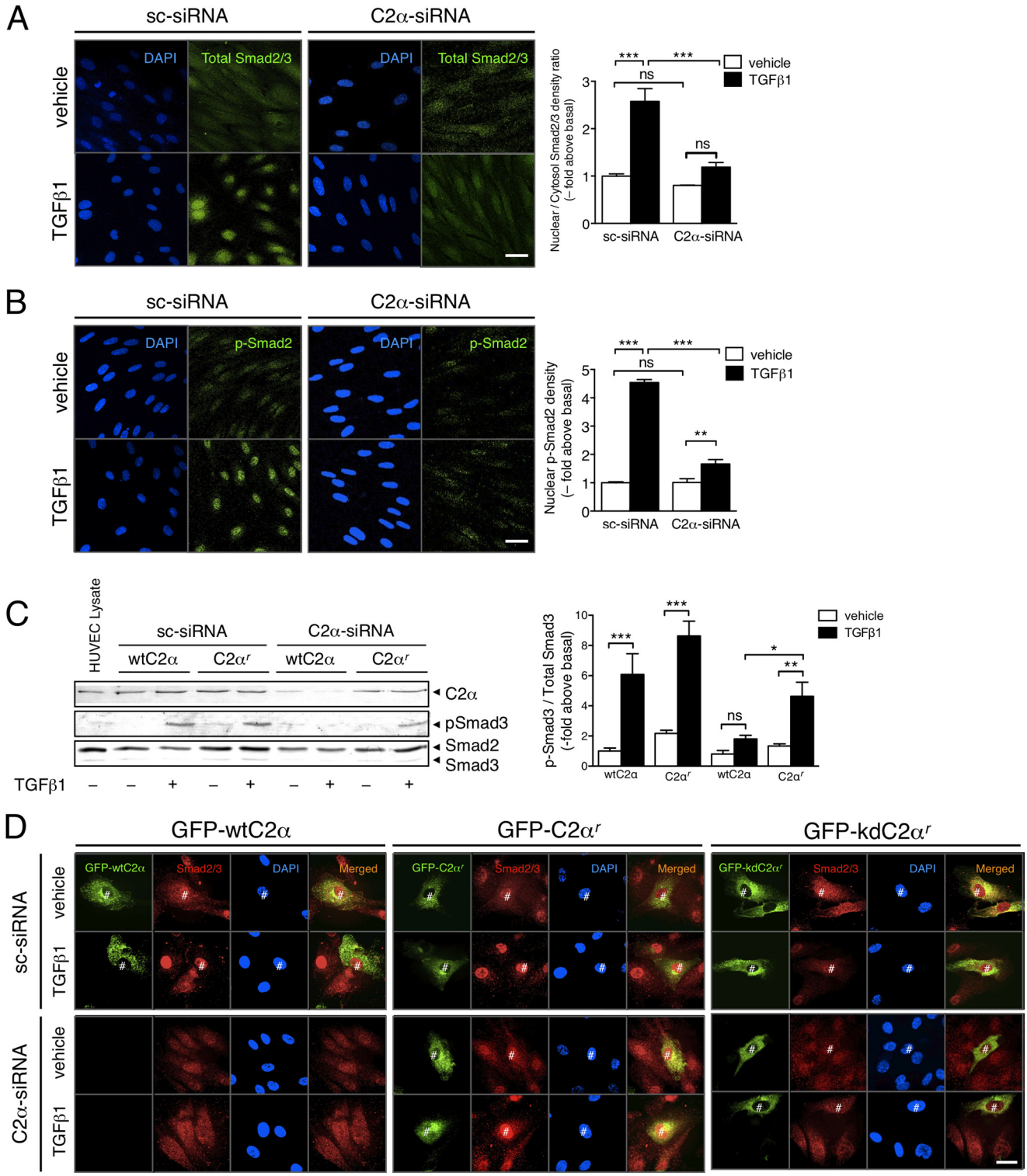

FIGURE 3. **TGFβ1-induced nuclear translocation of Smad2/3 depends on PI3K-C2α in EC.** *A* and *B*, immunofluorescent staining of Smad2/3 (*A*) and p-Smad3 (*B*) in TGFβ1-stimulated HUVECs. The cells were transfected with C2α#1 siRNA or sc-siRNA and stimulated with TGFβ1 (5 ng/ml) for 30 min, followed by anti-Smad2/3 antibody or anti-p-Smad3 antibody staining. Nuclei were stained by DAPI. *Left panels*, representative confocal images of the stained cells. *Right panels*, quantified data. The data were obtained from 48 cells per group. *Scale bar*, 20 μm. *C*, HUVECs were transfected with either wtC2α or C2α-siRNA-resistant C2α (C2α^r) and either C2α#1 siRNA or sc-siRNA. The cells were stimulated with TGFβ1 (5 ng/ml) for 30 min, followed by immunoblot analysis for p-Smad3. *Left panel*, representative blots. *Right panel*, quantified data ($n = 3$). *D*, HUVECs were transfected with either GFP-wtC2α, GFP-C2α^r, or GFP-tagged kinase deficient mutant of C2α^r (GFP-kdC2α^r) and either C2α-specific siRNA or sc-siRNA. The cells were stimulated with TGFβ1 (5 ng/ml) for 30 min, followed by immunofluorescent staining with anti-Smad2/3. Nuclei were stained by DAPI. *Scale bar*, 20 μm. #, transfected cells.

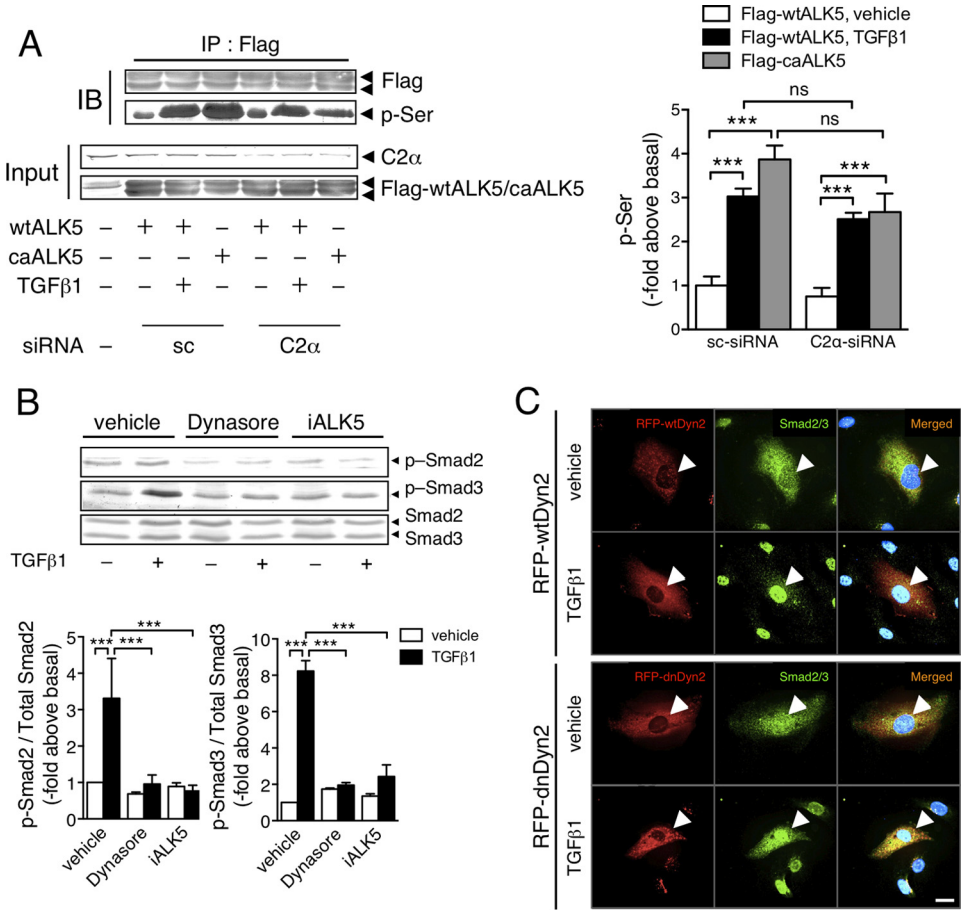

FIGURE 4. **TGFβ signaling requires PI3K-C2α distally to TGFβ1-induced ALK5 phosphorylation and endocytosis.** *A*, effects of C2α depletion on TGFβ1-induced ALK5 phosphorylation. *Left panel*, representative blots. *Right panel*, quantified data. HEK293T cells were transfected with either FLAG-wtALK5 or FLAG-caALK5 and either C2α#1 siRNA or sc-siRNA. The cell lysates were immunoprecipitated with anti-Flag antibody, followed by immunoblotting (*IB*) using anti-Flag and anti-phosphoserine (*p-Ser*) antibodies. A portion of the cell lysates was analyzed for the expression of the indicated proteins with IB. *IP*, immunoprecipitation. The data are from three-independent experiments, which yielded comparable results, and are expressed as multiples over the values in wtALK5 expressed in sc-siRNA-transfected cells. *B*, effects of the endocytosis inhibitor dynasore and the ALK5 inhibitor (*iALK5*) on TGFβ1induced-Smad3 phosphorylation. The cells were prepretreated or not with dynasore (80 μM) or ALK5 inhibitor (5 μM) for 30 min and stimulated with TGFβ1 (5 ng/ml) for 30 min ($n = 5$). *C*, effects of the expression of RFP wild-type dynamin2 (RFP-wtDyn2) or RFP dominant negative dynamin2 (RFP-dnDyn2) on TGFβ1-induced nuclear translocation of Smad2/3. The cells were transfected with the RFP-wtDyn2 or RFP-dnDyn2 expression vectors and stimulated with TGFβ1 (5 ng/ml) for 30 min, followed by anti-Smad2/3 immunostaining. Nuclei were stained by DAPI. The *arrowheads* denote the transfected cells. *Scale bar*, 20 μm.

TGFβ1-induced TGFβ Receptor Internalization into SARA-containing Endosomes Is Dependent on PI3K-C2α—TGFβ1 stimulation induced an increase in serine phosphorylation of ALK5 in HEK293T cells transfected with wtALK5 (Fig. 4*A*). In HEK293T cells, we observed PI3K-C2α dependence of TGFβ1-induced Smad2/3 phosphorylation (data not shown). PI3K-C2α knockdown did not inhibit TGFβ-induced serine phosphorylation of wtALK5, implying that PI3K-C2α is necessary for the TGFβ receptor signaling step, which is distal to phosphorylation of type I TGFβ receptor. Previous studies (28–31) showed that TGFβ1 stimulation triggered clathrin-dependent endocytosis of TGFβ receptor and that TGFβ receptor endocytosis was required for TGFβ activation of Smad2/3 signaling. We tested the effect of dynasore, an inhibitor of dynamin that is necessary for clathrin-dependent endocytosis, in EC. Treatment of HUVECs with dynasore abolished TGFβ1-induced phosphorylation of Smad2/3, like an ALK inhibitor (Fig. 4*B*). Likewise, the expression of the dominant negative dynamin2 mutant but not wild-type dynamin2 inhibited nuclear translocation of Smad2/3 (Fig. 4*C*). These observations suggested that TGFβ receptor endocytosis was required for Smad2/3 signaling. TGFβ1 stimulation promoted the internalization of type I TGFβ receptor ALK5 into the intracellular compartment, which was prevented by PI3K-C2α knockdown (Fig. 5*A*). Likewise, dynasore suppressed TGFβ1-induced ALK5 internalization. In these immunostainings, the anti-ALK5 antibody stained nuclei. ALK5 knockdown did not abolish or reduce the nuclear staining in anti-ALK5 immunostaining (Fig. 5*B*), suggesting that the nuclear staining was nonspecific. In sc-siRNA-transfected HUVECs, the expression of kdC2α^r partially inhibited TGFβ1-induced ALK5 internalization, differently from that of wtC2α^r expression (Fig. 5*C*). In C2α-siRNA-transfected HUVECs, the expression of kdC2α^r did not restore TGFβ1-induced ALK5 internalization. Double immunofluorescent staining of ALK5 and the early endosome marker EEA1 showed that TGFβ1 induced the internalization of ALK5 into the EEA1-positive early endosomes (Fig. 5*D*). PLA staining to detect interaction or close co-localization of two molecules showed that TGFβ1 stimulation induced the close co-localization of ALK5 and EEA1 (Fig. 5*E*, *green dots*), which was nearly abolished by PI3K-C2α knockdown.

Because SARA is located in the early endosomes and acts as a scaffold for Smad2/3 phosphorylation by ALK5 (28–30), we studied the requirement of SARA for TGFβ/ALK5 signaling, the possible co-localization of TGFβ1 receptors and SARA, and the effect of PI3K-C2α knockdown on the co-localization. Knockdown of SARA nearly completely suppressed TGFβ-induced Smad2/3 phosphorylation (Fig. 6*A*), indicating that SARA is essential for TGFβ/ALK5 signaling in HUVECs. Dou-

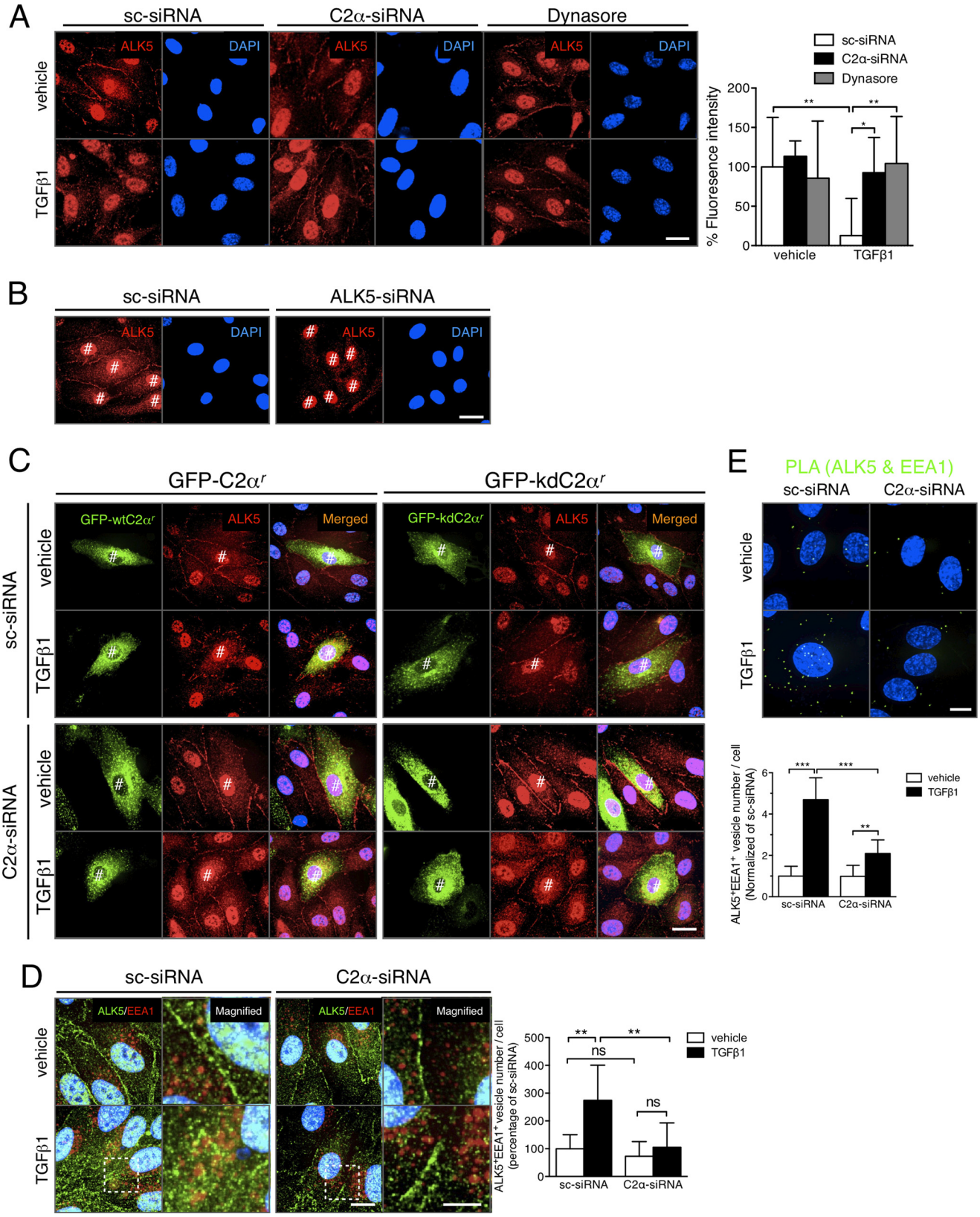

ble immunofluorescent staining using anti-SARA and anti-EEA1 showed that SARA was localized mainly in the EEA1-positive early endosome compartment in sc-siRNA-transfected HUVECs (Fig. 6*B*). TGFβ1 increased the SARA- and EEA1-double positive endosomes. PI3K-C2α knockdown did not affect the numbers of either SARA-positive or EEA1-positive vesicles in nonstimulated cells but abolished TGFβ1-induced increase in SARA- and EEA1-double positive early endosomes. PLA staining for ALK5 and SARA, combined with anti-EEA1 immunostaining, showed that TGFβ1 stimulation induced the close co-localization of ALK5 and SARA and that a portion of the closely co-localized ALK5 and SARA existed in the EEA1-positive early endosomes (Fig. 6*C*). Knockdown of PI3K-C2α inhibited the close co-localization of ALK5 and SARA in EEA1-positive early endosomes. These observations indicate that PI3K-C2α is involved in TGFβ1-induced ALK5 internalization into the SARA-containing endosomes through its kinase activity.

Endosomal Enrichment of PtdIns(3)P and Localization of SARA Are Not Dependent on PI3K-C2α—PI3K-C2α was previously reported to generate PtdIns(3)P and PtdIns(3,4)P_2 *in vivo* (8, 12–14). Because SARA is localized in early endosomes by binding PtdIns(3)P through its FYVE domain, we studied the effects of knockdown of PI3K-C2α and other PtdIns(3)P-producing PI3K on the cellular level and localization of PtdIns(3)P and PtdIns(3,4)P_2 by observing GFP fluorescence of HUVECs that had been transfected with the expression vectors for the PtdIns(3)P-specific probe GFP-$FYVE^{SARA}$ or the PtdIns(3,4)P_2-specific probe GFP-PH^{TAPP1}. In sc-siRNA-transfected nonstimulated HUVECs, the GFP-$FYVE^{SARA}$ signal was a punctate pattern as reported previously in nonendothelial cells (29) (Fig. 7*A*), suggesting that PtdIns(3)P was enriched in endosomes. TGFβ1 stimulation did not change GFP-$FYVE^{SARA}$ signal. Among three PI3Ks, knockdown of PI3K-C2α did not affect GFP-$FYVE^{SARA}$ signal. In contrast, that of either PI3K-C2β or Vps34 obviously reduced the density of vesicular GFP-$FYVE^{SARA}$ signals. Consistent with these observations, knockdown of either PI3K-C2β or Vps34 reduced anti-SARA-positive endosomes unlike PI3K-C2α knockdown and augmented the diffuse cytosolic anti-SARA staining (Fig. 7*B*), suggesting that PI3K-C2β and Vps34 but not PI3K-C2α generate PtdIns(3)P in SARA-containing endosomes. Thus, PI3K-C2α seems to participate in TGFβ-induced signaling, without altering the endosomal distribution of SARA.

In contrast to the effects on PtdIns(3)P level, TGFβ1 induced a rapid increase in GFP-PH^{TAPP1} signal in lamellipodia (Fig. 7*C* and supplemental Movies S1 and S2), suggesting a localized increase in the membrane PtdIns(3,4)P_2 level in TGFβ1-stimulated cells. Notably, PI3K-C2α knockdown abolished TGFβ1-induced increase in GFP-PH^{TAPP1} signals, indicating that PI3K-C2α is involved in the generation of PtdIns(3,4)P_2 in lamellipodia. The recent study implicated PI3K-C2α-generated PtdIns(3,4)P_2 in endocytosis (14). Therefore, it is an interesting possibility that PI3K-C2α is involved in TGFβ1-induced endocytosis of TGFβ receptor through forming PtdIns(3,4)P_2 in the plasma membrane.

PI3K-C2α Is Required for SARA-Smad2/3 Complex Formation—Because SARA is associated with Smad2/3 and acts as a scaffold for Smad2/3 phosphorylation by type I TGFβ receptor ALK5, we studied the PI3K-C2α dependence of SARA-Smad2/3 complex formation, using anti-SARA immunoprecipitation and the following anti-Smad2/3 immunoblotting. For the experiments, we employed HEK293T cells for efficiency of gene transduction. We co-transfected HEK293T cells with the expression vectors for either wtSARA or the ΔSBD-SARA and either wtALK5 or caALK5, with or without Smad2/3 expression vectors. We detected co-immunoprecipitation of Smad2/3 in the anti-SARA immunoprecipitates in the cells transfected with Smad2/3, wtSARA, and wtALK5. However, without Smad2/3 transfection, we did not detect Smad2/3 in the anti-SARA immunoprecipitates (Fig. 8*A*). In sc-siRNA-treated control cells that had been transfected with wtSARA and wtALK5, we detected the association of Smad3 and Smad2 with SARA (Fig. 8, *B* and *C*). The expression of caALK5 substantially stimulated the association of Smad3 and Smad2 with SARA and resultant phosphorylation of Smad3 and Smad2, which were both markedly inhibited by the expression of ΔSBD-SARA. In contrast, in PI3K-C2α-depleted cells, caALK5 expression barely stimulated the association of Smad3 and Smad2 with SARA and phosphorylation of Smad3 and Smad2. Thus, PI3K-C2α is required for ALK5-mediated formation of the SARA and Smad2/3 complex and phosphorylation of Smad2/3.

We also studied the interaction of endogenous SARA and Smad2/3 in HUVECs using PLA staining. TGFβ1 promoted SARA-smad2/3 interaction in the endosomes in sc-siRNA-transfected control HUVECs. A portion of the PLA signal was co-localized with EEA1, indicating that SARA and Smad2/3 complex were located in the early endosomes. PI3K-C2α knockdown inhibited TGFβ1-stimulated SARA-smad2/3 interaction (Fig. 8*D*). The observations indicate that TGFβ1 stimulation of the

FIGURE 5. **PI3K-C2α is required for TGFβ1-induced internalization of TGFβ receptor into the early endosomes in EC.** *A*, effects of C2α depletion or dynasore on TGFβ1-induced internalization of endogenous ALK5. The cells were either transfected with C2α#1 siRNA or sc-siRNA or pretreated with dynasore (80 μM) for 30 min and stimulated with TGFβ1 (5 ng/ml) for 30 min. *Left panel*, representative confocal images of the stained cells. *Right panel*, quantified data of fluorescence intensity per cell that were obtained from 24 cells per group. Nuclei were stained by DAPI. *Scale bar*, 20 μm. *B*, effects of ALK5 knockdown on the nuclear staining in anti-ALK5 immunostaining. HUVECs were transfected with ALK5-specific siRNA (ALK5-siRNA) or sc-siRNA, followed by anti-ALK5 immunofluorescent staining. Nuclei were stained by DAPI. *Scale bar*, 20 μm. #, nonspecific nuclear signals. *C*, effects of the expression of a kinase-deficient C2α mutant on TGFβ1-induced ALK5 internalization. HUVECs were transfected with either GFP-C2α^r or GFP-kdC2α^r and either C2α#1 siRNA or sc-siRNA. The cells were stimulated with TGFβ1 (5 ng/ml) for 30 min, followed by immunofluorescent staining with anti-ALK5 antibody. Nuclei were stained by DAPI. #, transfected cells. *D*, double immunofluorescent staining of ALK5 (*green*) and EEA1 (*red*) in TGFβ1-stimulated HUVECs. The cells were transfected with C2α#1 siRNA or sc-siRNA and stimulated with TGFβ1 (5 ng/ml) for 30 min. *Left panel*, representative confocal images of the stained cells. Magnified views of the *boxed areas* are also shown. Nuclei were stained by DAPI. *Scale bar*, 20 μm. *Right panel*, quantified data of the ALK5/EEA1-double positive vesicle numbers per cell that were obtained from 24 cells per group. *E*, PLA staining of ALK5 and EEA1 (*green*) in TGFβ1-stimulated HUVECs. The cells were transfected with C2α#1 siRNA or sc-siRNA and stimulated with TGFβ1 (5 ng/ml) for 30 min. Nuclei were stained by DAPI. *Upper panel*, representative confocal images of the stained cells. *Scale bar*, 20 μm. *Lower panel*, quantified data of the numbers of ALK5/EEA1 interactions per cell that were obtained from 24 cells per group.

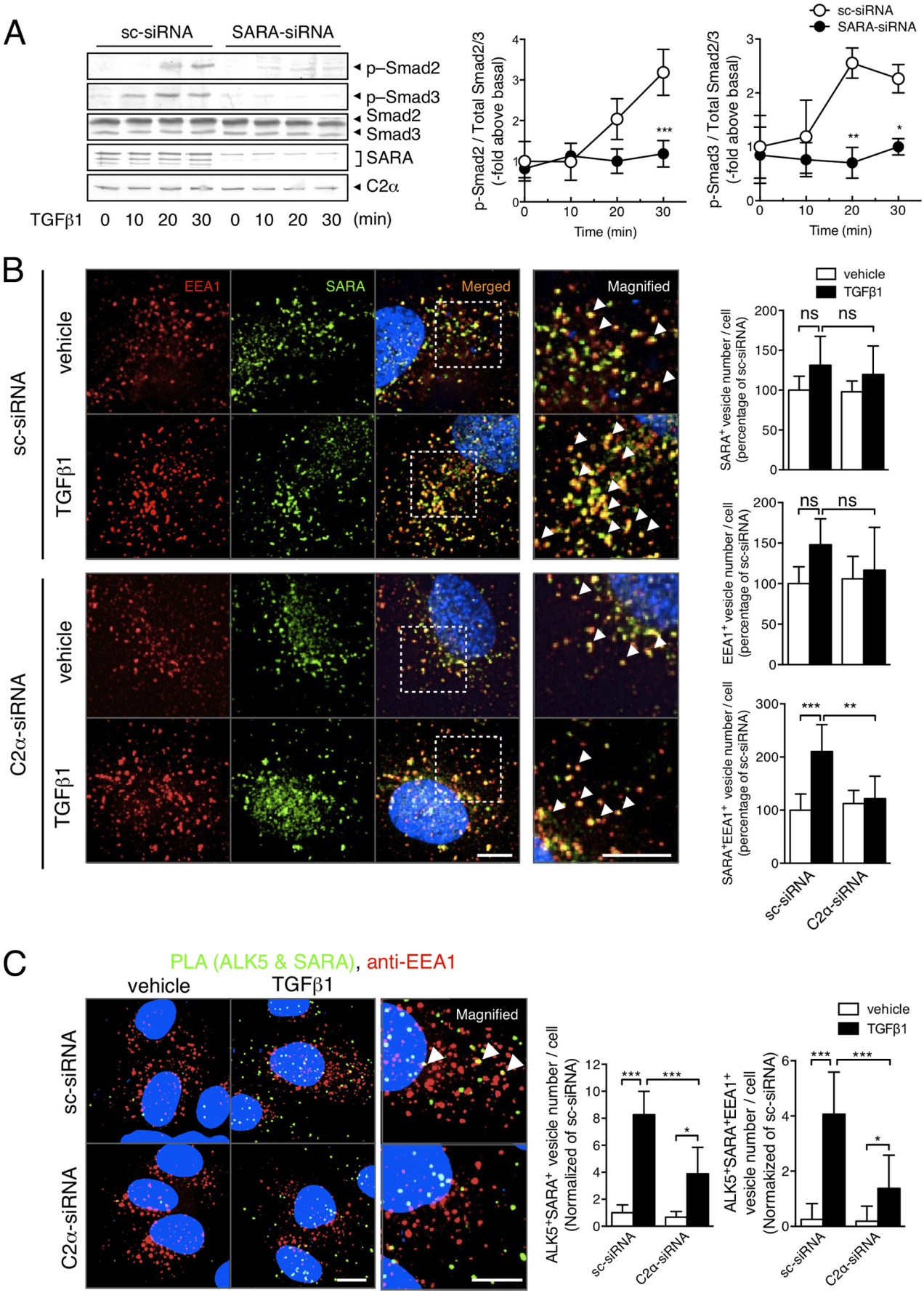
A
sc-siRNA
SARA-siRNA
p–Smad2
p–Smad3
Smad2
Smad3
SARA
C2α
TGFβ1 0 10 20 30 0 10 20 30 (min)
p-Smad2 / Total Smad2/3 (-fold above basal)
Time (min)
sc-siRNA
SARA-siRNA
p-Smad3 / Total Smad2/3 (-fold above basal)
Time (min)
B
EEA1
SARA
Merged
Magnified
sc-siRNA
C2α-siRNA
vehicle
TGFβ1
vehicle
TGFβ1
SARA+ vesicle number / cell (percentage of sc-siRNA)
EEA1+ vesicle number / cell (percentage of sc-siRNA)
SARA+EEA1+ vesicle number / cell (percentage of sc-siRNA)
ns
sc-siRNA
C2α-siRNA
C
PLA (ALK5 & SARA), anti-EEA1
vehicle
TGFβ1
Magnified
sc-siRNA
C2α-siRNA
ALK5+SARA+ vesicle number / cell (Normalized of sc-siRNA)
ALK5+SARA+EEA1+ vesicle number / cell (Normakized of sc-siRNA)
vehicle
TGFβ1
sc-siRNA
C2α-siRNA

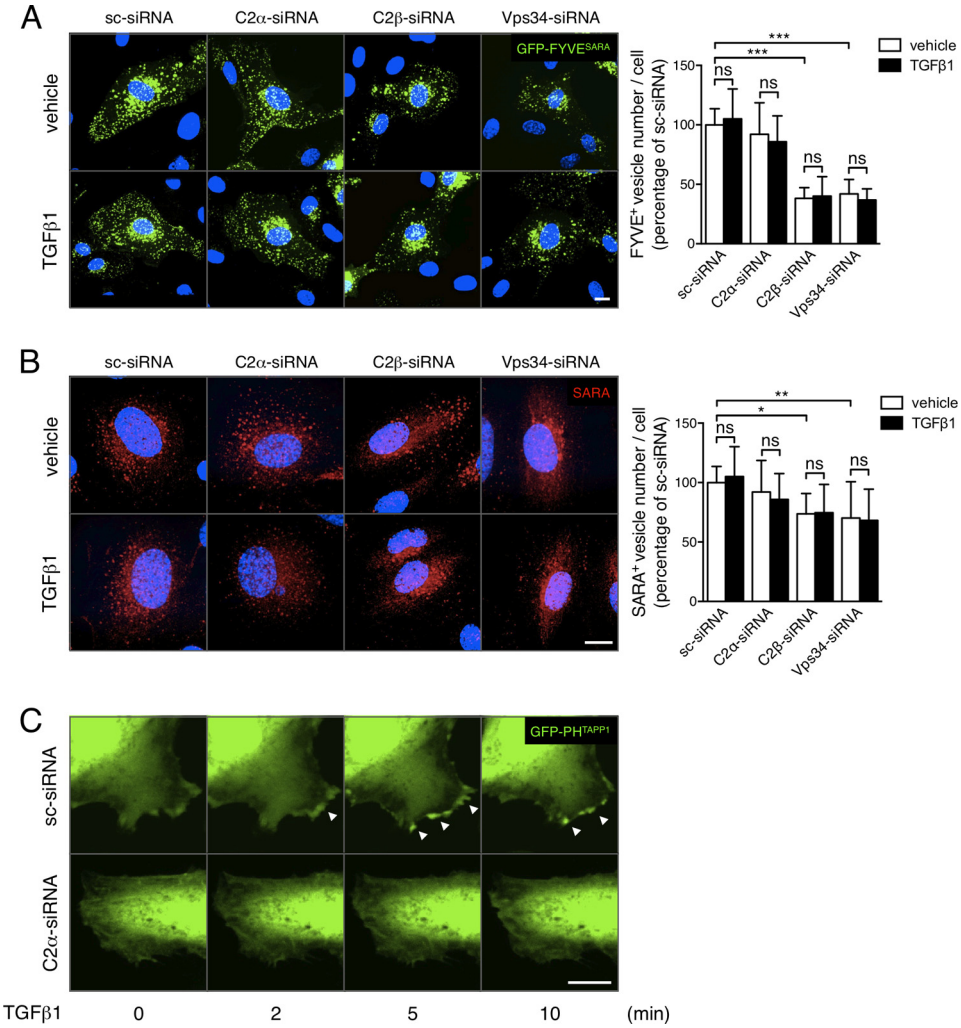

FIGURE 7. **PI3K-C2α is not required for PtdIns(3)P enrichment or the localization of SARA in the endosomes but for TGFβ-induced increase in PtdIns(3,4)P2 in lamellipodia.** *A*, GFP-FYVE^{SARA} fluorescence. The HUVECs were co-transfected with the GFP-FYVE^{SARA} expression vector and either C2α#1 siRNAs or sc-siRNA and stimulated with TGFβ1 (5 ng/ml) for 30 min or left untreated. Nuclei were stained by DAPI. *Left panel*, representative confocal images. *Right panel*, quantified data of the numbers of GFP-FYVE fluorescence-positive vesicles per cell that were obtained from 48 cells per group. *B*, anti-SARA immunofluorescent staining. The HUVECs were transfected with either C2α-siRNAs or sc-siRNA and stimulated with TGFβ1 (5 ng/ml) for 30 min or left untreated. Nuclei were stained by DAPI. *Left panel*, representative confocal images. *Right panel*, quantified data of anti-SARA-positive vesicles per cell that were obtained from 48 cells per group. *Scale bar*, 20 μm. *C*, GFP-PH^{TAPP1} fluorescence. The HUVECs were co-transfected with the GFP-PH^{TAPP1} expression vector and either C2α-siRNAs or sc-siRNA and stimulated with TGFβ1 (5 ng/ml) for 30 min or left untreated. Nuclei were stained by DAPI. Confocal images at 2, 5, and 10 min after the additions of TGFβ1 or vehicle are shown.

interaction of endogenous SARA and Smad2/3 in the endosomes requires PI3K-C2α in HUVECs.

PI3K-C2α Is Required for TGFβ1-induced VEGF-A Expression in EC—Consistent with previous studies (38–41), TGFβ1 increased the expression of mRNA and protein of VEGF-A in control HUVECs (Fig. 9, *A–C*). The stimulatory effects of TGFβ1 were inhibited by knockdown of the common Smad Smad4, suggesting the involvement of Smad2/3. Furthermore, TGFβ1-induced VEGF-A expression was abolished by the pharmacological blockade of ALK5 (Fig. 9*D*). These observations together suggested that TGFβ1-induced VEGF-A up-regulation was dependent on the ALK5-Smad pathway. In agreement with the involvement of the canonical Smad pathway in TGFβ1-induced VEGF-A expression, knockdown of PI3K-C2α, but not PI3K-C2β, p110α, or Vps34, inhibited TGFβ1-induced VEGF-A expression (Fig. 9, *A–C*). Moreover, treat-

FIGURE 6. **PI3K-C2α is required for TGFβ receptor internalization into SARA-containing endosomes in EC.** *A*, effects of SARA depletion on TGFβ1-induced Smad2/3 phosphorylation in HUVECs. The cells were transfected with SARA-specific siRNA or sc-siRNA. Serum-starved cells were stimulated with TGFβ1 (5 ng/ml) for the indicated time periods and subjected to immunoblot analysis for p-Smad2, p-Smad3, and total Smad2 and Smad3. *Left panel*, representative blots. *Right panel*, quantified data ($n = 3$). *B*, double immunofluorescent staining of EEA1 (*red*) and SARA (*green*) in TGFβ1-stimulated HUVECs. The cells were transfected with C2α#1 siRNA or sc-siRNA and stimulated with TGFβ1 (5 ng/ml) for 30 min. Nuclei were stained by DAPI. *Right panel*, quantified data of the numbers of SARA (*upper panel*), EEA1 (*middle panel*), and SARA/EEA1-double (*lower panel*) positive vesicle numbers per cell that were obtained from 48 cells per group. *Scale bar*, 20 μm. *C*, PLA staining (*green*) of ALK5 and SARA and anti-EEA1 immunostaining (*red*) in TGFβ1-stimulated HUVECs. The cells were transfected with C2α#1 siRNA or sc-siRNA and stimulated with TGFβ1 (5 ng/ml) for 30 min. *Left panel*, representative confocal images of the stained cells. *Green* and *red* denote PLA signals and immunostaining signals, respectively. Nuclei were stained by DAPI. *Scale bar*, 20 μm. *Right panel*, quantified data of the numbers of PLA signals (*left graph*) and PLA signal/anti-EEA1-double positive vesicle numbers per cell (*right graph*) that were obtained from 24 cells per group.

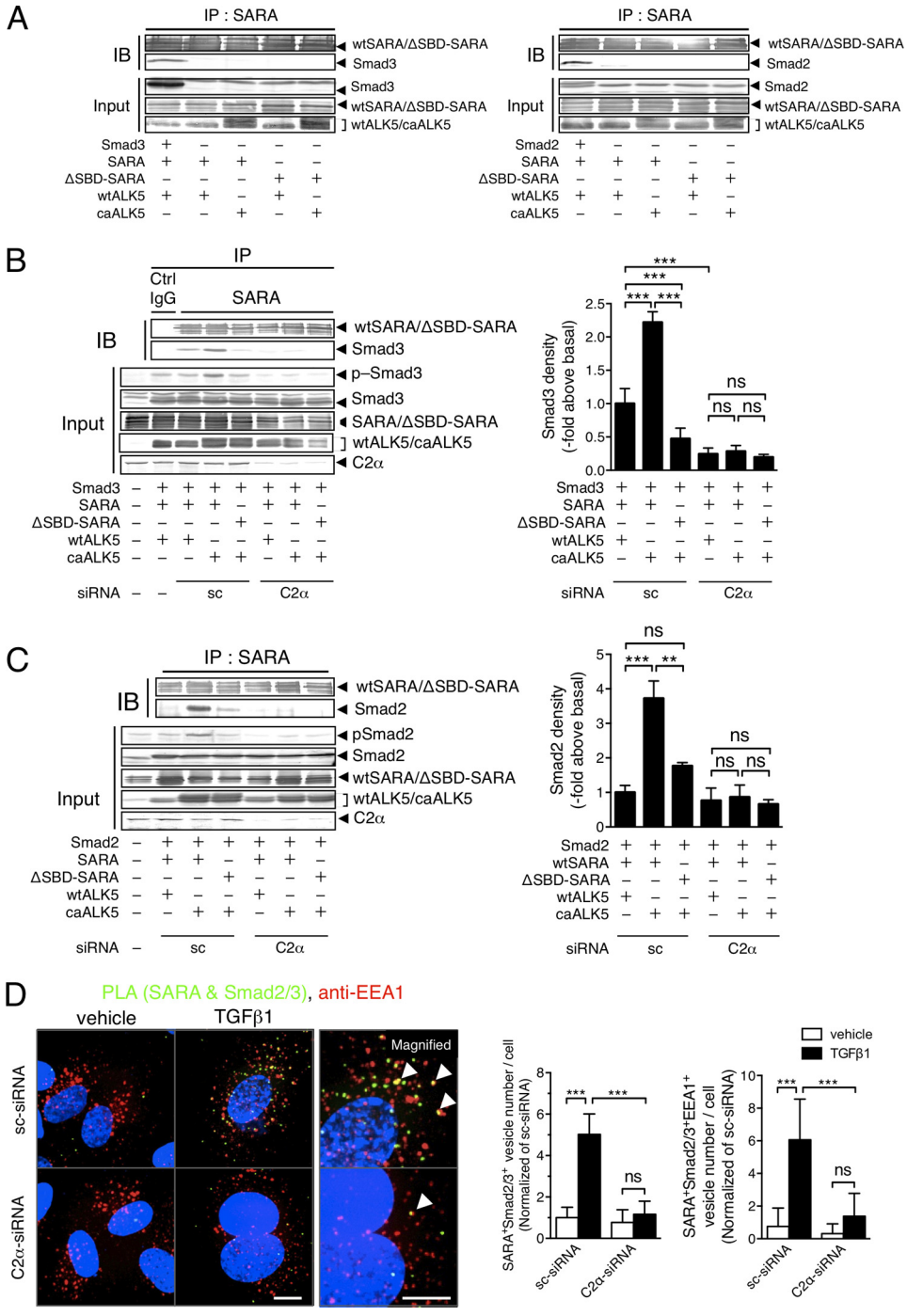

FIGURE 8. **SARA-Smad3 complex formation is dependent on PI3K-C2α.** *A–C*, analyses of complex formation between SARA and Smad2/3 by co-immunoprecipitation-immunoblotting in HEK293T cells. *A*, the cells were transfected with the expression vectors for either wtSARA or ΔSBD-SARA and either wtALK5 or caALK5, with or without Smad2/3 expression vectors. The cell lysates were immunoprecipitated with anti-SARA antibody, followed by immunoblotting (*IB*) using anti-SARA, anti-Smad3, or anti-Smad2 antibody. *B* and *C*, the cells were co-transfected with the expression vectors for either Smad2 or Smad3, either wtSARA or ΔSBD-SARA, either wtALK5 or caALK5, and either C2α#1 siRNA or sc-siRNA. The cell lysates were immunoprecipitated with anti-SARA antibody, followed by immunoblotting using anti-SARA, anti-Smad3 antibody in *B*, and anti-Smad2 antibody in *C*. Portions of the cell lysates were analyzed for the expression of the indicated proteins with immunoblotting (*Input*). *IP*, immunoprecipitation; *Ctrl*, control. *Left panel*, representative blots. *Right panel*, quantified data of the amounts of Smad3 and Smad2 in immunoprecipitates from the cells transfected as indicated. The data are means ± S.E. from four independent experiments, which yielded comparable results, and expressed as multiples over the values in wtALK5- and sc-siRNA-transfected cells. *D*, PLA staining of SARA and Smad2/3 (*green*) and anti-EEA1 immunostaining (*red*) in TGFβ1-stimulated HUVECs. The cells were transfected with C2α#1 siRNA or sc-siRNA and stimulated with TGFβ1 (5 ng/ml) for 30 min. *Left panel*, representative confocal images of the stained cells. *Green* and *red* denote PLA signals and immunostaining signals, respectively. Nuclei were stained by DAPI. *Scale bar*, 20 μm. *Right panel*, quantified data of the numbers of PLA signals (*left graph*) and PLA signal/anti-EEA1 staining-double positive vesicle numbers per cell (*right graph*) that were obtained from 24 cells per group.

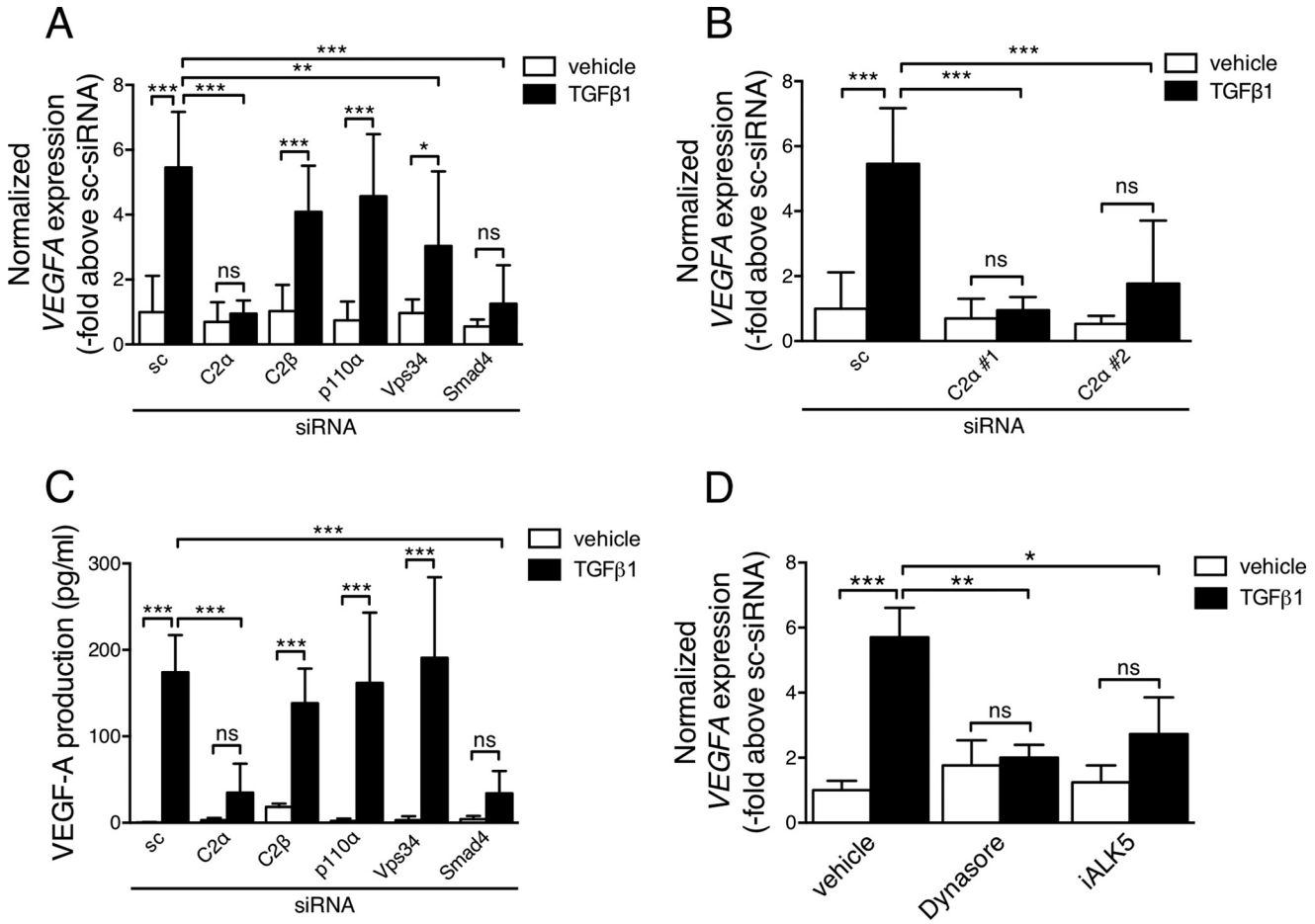

FIGURE 9. **PI3K-C2α is required for TGFβ1-induced, Smad-dependent VEGF-A production in EC.** HUVECs were transfected with either of C2α(#1), C2β, p110α, Vps34, and Smad4-specific siRNA or sc-siRNA and stimulated with TGFβ1 in the presence and absence of the indicated inhibitors. *A*, VEGF-A (*VEGFA*) mRNA expression in the cells stimulated with TGFβ1 (5 ng/ml) for 6 h. The *VEGFA* mRNA expression levels were determined with real time PCR and were corrected for 18 S rRNA level ($n = 6$). *B*, *VEGFA* mRNA expression in the cells were transfected with either of C2α#1, C2α#2, and sc-siRNA and stimulated with TGFβ1 (5 ng/ml) for 6 h. The *VEGFA* mRNA expression levels were determined with real time PCR and were corrected for 18 S rRNA level ($n = 3$). *C*, VEGF-A peptide concentrations in the media of the cells stimulated with TGFβ1 (5 ng/ml) for 12 h ($n = 3$). *D*, effects of dynasore and ALK5 inhibitor on *VEGFA* mRNA expression. The cells were prepretreated or not with dynasore (80 μM) or iALK5 (5 μM) for 30 min and stimulated with TGFβ1 (5 ng/ml) for 6 h ($n = 5$). In *A–D*, the data are expressed as multiples over the values in TGFβ1-nonstimulated sc-siRNA-transfected or vehicle-treated control cells.

ment of HUVECs with dynasore abolished TGFβ1-induced VEGF-A mRNA expression with suppression of Smad3 phosphorylation (Figs. 4*B* and 9*C*). These findings indicate that PI3K-C2α- and endocytosis-dependent Smad2/3 signaling mediates TGFβ-induced VEGF-A expression in EC.

PI3K-C2α Is Required for TGFβ1-induced Endothelial Cell Migration, Tube Formation, and in Vivo Angiogenesis—In a wound healing assay, PI3K-C2α knockdown inhibited migration of HUVECs induced by either TGFβ1 or VEGF-A (Fig. 10, *A* and *B*). The ALK5 inhibitor suppressed TGFβ1-induced cell migration. Interestingly, the inhibitor of VEGFR2 suppressed not only VEGF-induced but also TGFβ1-induced cell migration, indicating that TGFβ1-induced cell migration is dependent on VEGFR2. Likewise, PI3K-C2α knockdown inhibited tube formation induced by either TGFβ1 or VEGF-A (Fig. 10, *C* and *D*). The inhibition of VEGF-A-induced tube formation by PI3K-C2α knockdown is most likely because VEGFR2 signaling is dependent on PI3K-C2α as we demonstrated previously (8). The ALK5 inhibitor and the VEGFR2 inhibitor blocked TGFβ1-induced tube formation (Fig. 10, *E* and *F*). In addition, dynasore suppressed TGFβ1-induced tube formation. These observations suggest that TGFβ1-induced, ALK5-mediated stimulation of endothelial migration and morphogenesis is dependent on stimulation of VEGF-A expression and VEGFR2 signaling, in which PI3K-C2α and the endocytic process are involved.

We finally investigated a role for PI3K-C2α in *in vivo* angiogenesis, using a Matrigel plug assay in conditional PI3K-C2α knock-out mice. We subcutaneously injected Matrigel plug with or without TGFβ1 in mice with endothelial specific deletion of PI3K-C2α ($C2\alpha^{\Delta EC}$) or smooth muscle-specific PI3K-C2α deletion ($C2\alpha^{\Delta SMC}$) and compared angiogenesis in both mutant mice with that in control mice ($C2\alpha^{flox/flox}$). The inclusion of TGFβ1 in Matrigel increased the formation of anti-vWF-positive microvessels in Matrigel plugs in control mice, compared with vehicle (Fig. 11, *A–F*). In contrast, in $C2\alpha^{\Delta EC}$ mice TGFβ1 failed to stimulate microvessel formation. In $C2\alpha^{\Delta SMC}$ mice, however, TGFβ1 stimulated microvessel formation in Matrigel plugs to the similar extent as in control mice (Fig. 11, *D–F*). We performed double immunofluorescent staining of p-Smad2 and EC marker CD31 in Matrigels containing either TGFβ or vehicle that had been implanted in $C2a^{DEC}$

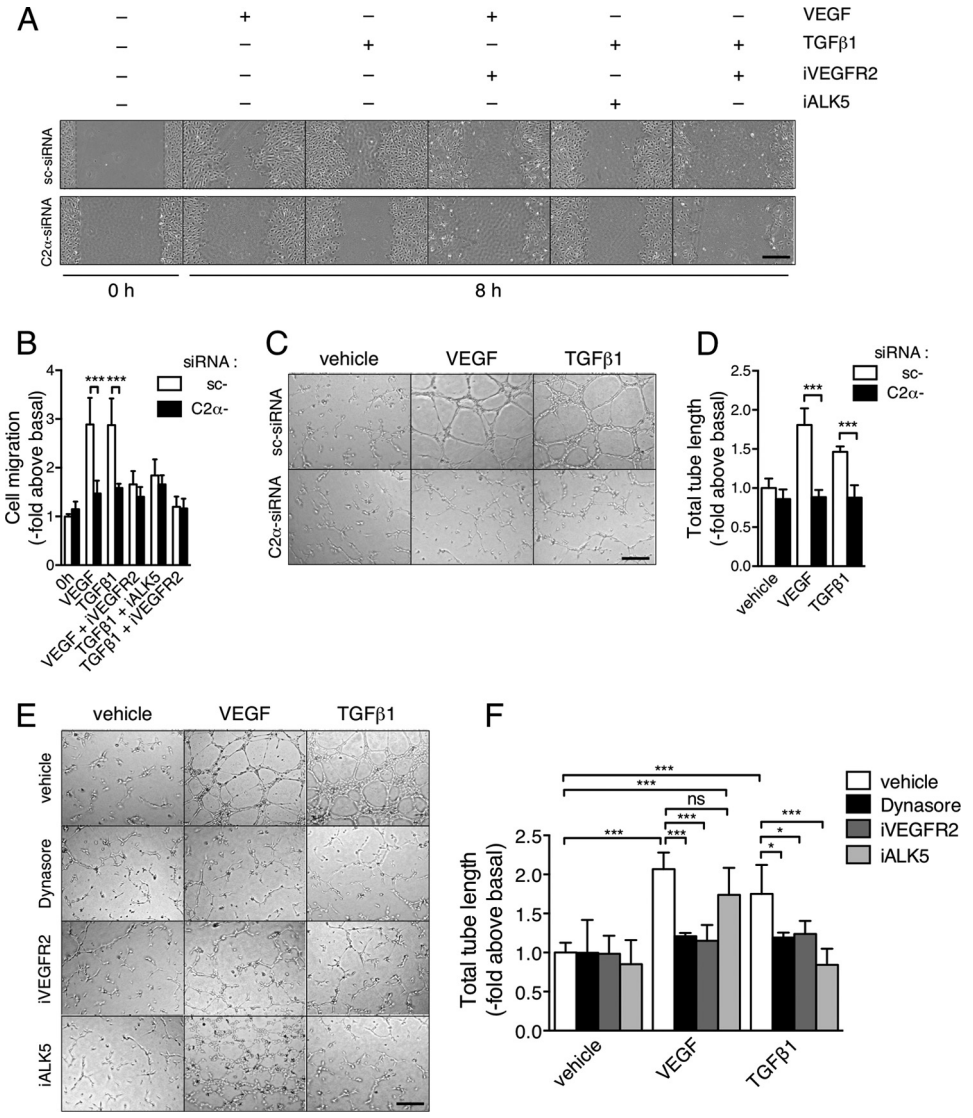

FIGURE 10. **TGFβ1-induced endothelial cell migration and tube formation are VEGFR2-mediated and PI3K-C2α-dependent.** *A* and *B*, effects of inhibitors of VEGFR2 and ALK5 on TGFβ1- and VEGF-induced cell migration. HUVECs were stimulated with TGFβ1 (5 ng/ml) or VEGF (50 ng/ml) in the presence and absence of iALK5 (5 μM) and the VEGFR2 inhibitor (iVEGFR2) (10 μM). Cell migration was determined with scratch wounding healing assay. *A*, representative microscopic views. *B*, quantified data ($n = 4$). *C* and *D*, effects of C2α-knockdown on TGFβ1- and VEGF-induced tube formation. siRNA-transfected cells were stimulated with VEGF-A (50 ng/ml) or TGFβ1 (5 ng/ml) for 12 h. *C*, representative microscopic views; *D*, quantified data ($n = 4$). *E* and *F*, effects of dynasore (80 μM), iVEGFR2 (10 μM), and iALK5 (5 μM) on TGFβ1- and VEGF-induced tube formation. *E*, representative microscopic views. *F*, quantified data ($n = 4$).

and $C2a^{DSMC}$ mice. $C2a^{DEC}$ mice showed much reduced p-Smad2- and CD31-double positive cells compared with $C2a^{DSMC}$ (Fig. 11*G*), suggesting that Smad2 activation in EC was attenuated in $C2a^{DEC}$ mice. These observations suggest that TGFβ1-induced microvessel formation in Matrigel plugs is dependent on PI3K-C2α that is expressed in EC but not smooth muscle.

DISCUSSION

Accumulated evidence indicates that TGFβ receptor-Smad2/3 signaling is dependent on the endocytosis of the TGFβ receptor complex (28–31). Upon TGFβ binding, TGFβ receptors are internalized into early endosomes, where the Smad anchor SARA is enriched through its FYVE domain. SARA interacts with Smad2/3, facilitating Smad2/3 phosphorylation and thereby their nuclear translocation. PI3K may be involved in at least two steps of these TGFβ receptor signaling processes: TGFβ-induced TGFβ receptor internalization and the endosomal localization of SARA. In the present study, we identified class II PI3K-C2α as PI3K isoform that is engaged in TGFβ-induced activation of Smad2/3 signaling. Our data indicate that PI3K-C2α is required for the endocytosis of TGFβ receptor but not for endosomal localization of SARA.

The present observation in EC that TGFβ-induced Smad2/3 phosphorylation is dependent on TGFβ receptor internalization into the EEA1-positive, SARA-containing early endosomes (Figs. 4–6) is similar to the previous observations in other types of cells including HeLa cells, HepG2 cells, and Mv1Lu cells (28, 30, 31), although some discrepant results on the necessity of SARA for ALK5/Smad2/3 signaling were reported (42, 43). Either PI3K-C2α depletion (~80~90%) or the expression of the kinase-deficient Cα mutant strongly sup-

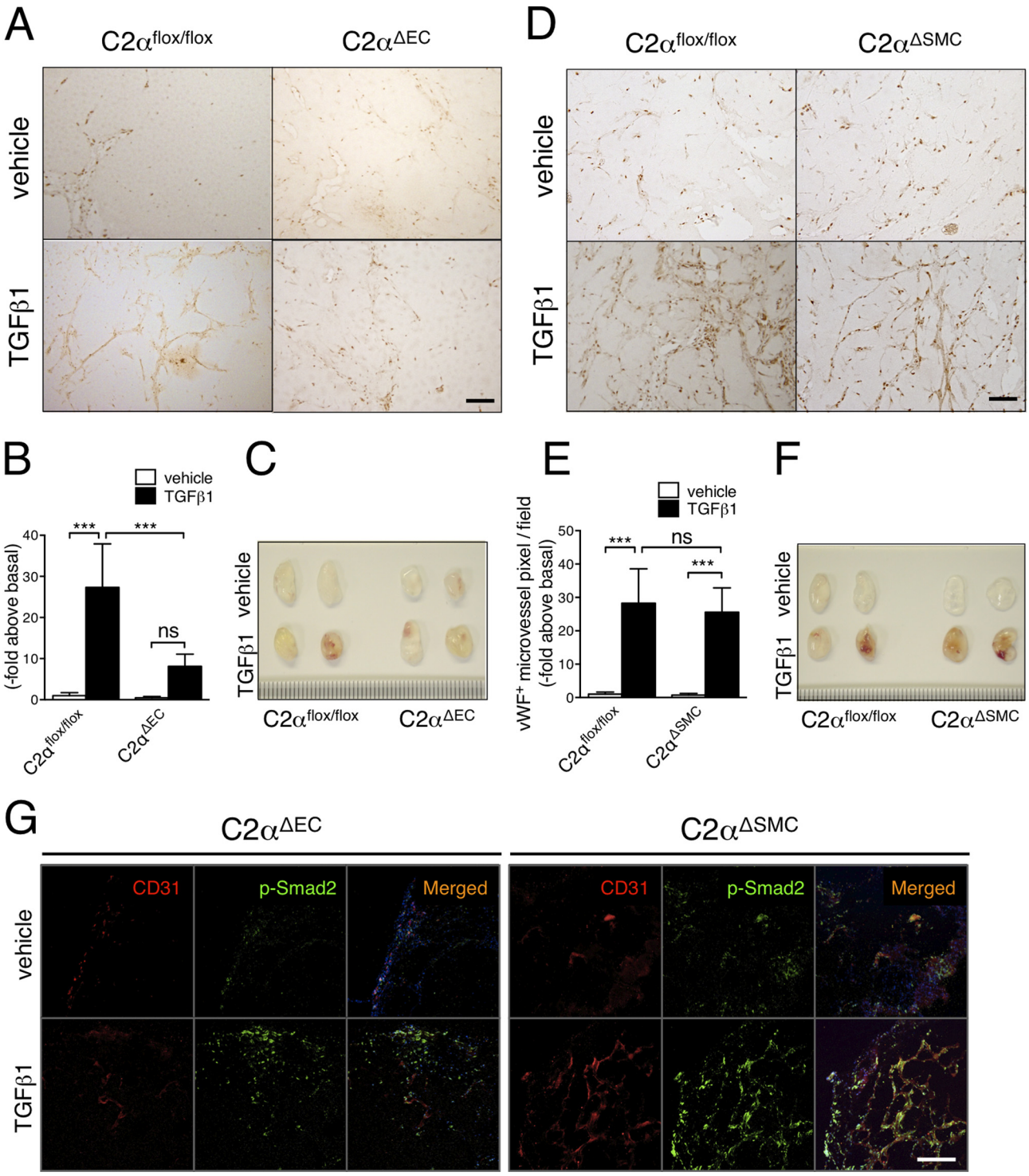

FIGURE 11. **Endothelial PI3K-C2α is necessary for TGFβ1-induced angiogenesis *in vivo*.** Matrigels containing PBS (vehicle) or TGFβ1 were injected into the subcutaneous tissues on the back of EC-specific C2α-deleted ($C2\alpha^{\Delta EC}$), SMC-specific C2α-deleted ($C2\alpha^{\Delta SMC}$), and control ($C2\alpha^{flox/flox}$) mice. Matrigel plugs were removed 10 days later and analyzed for microvascular formation by immunohistochemistry using anti-vWF antibody. *A* and *D*, representative views of anti-vWF immunostained sections of Matrigel plugs in $C2\alpha^{\Delta EC}$ (*A*) and $C2\alpha^{\Delta SMC}$ (*D*) mice. *B* and *E*, quantified data of neovessel formation in Matrigel plugs (seven mice per group). *C* and *F*, representative gross views of Matrigel plugs resected from mice. *G*, double immunofluorescent staining of CD31 (*red*) and p-Smad2 (*green*) in Matrigel plugs in $C2\alpha^{\Delta EC}$ (*left panel*) and $C2\alpha^{\Delta SMC}$ (*right panel*) mice. Nuclei were stained by DAPI. *Scale bar*, 50 μm.

pressed the internalization of TGFβ receptor, like the dynamin inhibitor dynasore (Fig. 5). Because either PI3K-C2α depletion or dynasore markedly inhibited TGFβ-induced Smad2/3 phosphorylation (Figs. 1, *B* and *C*, and 4*B*), there is a good correlation between TGFβ-induced TGFβ receptor internalization and Smad2/3 phosphorylation. As discussed in detail below, PI3K-C2α depletion did not compromise the endosomal distribution of the Smad anchor SARA. Based on these findings, it is reasonable to suggest that PI3K-C2α is involved in TGFβ receptor-activated Smad2/3 signaling largely through regulat-

ing TGFβ receptor internalization. In addition, the overexpression of wtC2α did not affect TGFβ-induced Smad2/3 activation or ALK5 internalization, suggesting that the endogenous level of wtC2α was sufficient for full activation of TGFβ receptor-induced Smad2/3 signaling.

We recently demonstrated in EC that ligand binding-triggered endocytosis of two different classes of cell surface receptors, VEGFR2 and $S1P_1$, was dependent on PI3K-C2α (8, 15). Interestingly, PI3K-C2α depletion inhibited only a part of multiple signaling pathways activated by VEGF and S1P: Rho activation in VEGF signaling and Rac activation in S1P signaling. We observed using FRET imaging technique that both VEGF-induced Rho activation and S1P-induced Rac activation occurred in PtdIns(3)P-enriched endosomes, as well as the plasma membrane. The present study together with those previous observations indicate that PI3K-C2α participates in signaling on the endosomes, upon the activation of different classes of receptors including receptor tyrosine kinases, G protein-coupled receptors, and receptor serine/threonine kinases. Thus, the ability of PI3K-C2α to regulate the endocytosis of different classes of cell surface receptors controls endosomal signaling.

A recent study (14) suggested a novel mechanism about a general role of PI3K-C2α in clathrin-dependent endocytosis in non-vascular cells; the formation of PtdIns(3,4)P_2 by PI3K-C2α at clathrin-coated pits and late endocytic intermediates before dynamin-mediated fission recruited the PtdIns(3,4)P_2–effector protein SNX9, promoting maturation of clathrin-coated pits toward endocytic vesicles. They suggested that PI3K-C2α formed PtdIns(3,4)P_2 from PtdIns(4)P, which was generated through 5′-dephosphorylation of PtdIns(4,5)P_2 enriched in the clathrin-coated pits. We observed that TGFβ1 induced the rapid and sustained formation of lamellipodia with a local lamellipodial increase in PtdIns(3,4)P_2 (Fig. 7*C*). In the lamellipodial region of the plasma membrane, endocytosis carries membrane-anchored Rho GTPases and integrins to the cell interior, and these molecules are recycled to the specific regions of the plasma membrane, which promotes lamellipodial protrusion (44). Considering the rapid onset of TGFβ1-induced lamellipodial formation and an increase in PtdIns(3,4)P_2 level, these responses very likely represent non-genomic effects of TGFβ1. It remains to be clarified how TGFβ induces a rapid increase in the level of PtdIns(3,4)P_2 through a mechanism involving PI3K-C2α in EC.

The interaction of the FYVE domain in SARA with PtdIns(3)P, a predominant phosphoinositide in the endosomes, serves the endosomal localization of SARA (28, 29, 45). Previous studies (12, 46) showed that PI3K-C2α formed PtdIns(3)P in cells. These observations together with the finding of the endosomal localization of PI3K-C2α (8) suggested that PI3K-C2α might be responsible for enrichment of PtdIns(3)P in the endosomes. However, the present study showed that PI3K-C2α depletion did not reduce PtdIns(3)-enriched endosomes (Fig. 7*A*). Instead, knockdown of either PI3K-C2β or Vps34 reduced PtdIns(3)-enriched endosomes. In agreement with these findings, knockdown of PI3K-C2β or Vps34 but not PI3K-C2α reduced SARA-containing vesicles (Fig. 7*B*). Our observations of the effects of PI3K-C2β and Vps34 depletion on SARA distribution are consistent with the previous reports showing that the nonselective PI3K inhibitor wortmannin totally changed the endosomal localization of SARA to a diffuse cytosolic pattern with inhibition of Smad signaling at the relatively low concentrations of 50–100 nM (29, 45). This range of concentration of wortmannin does not effectively inhibit PI3K-C2α because PI3K-C2α is relatively resistant to wortmannin compared with the other PI3K (5, 7, 47). Thus, PI3K-C2α is not a major enzyme to be responsible for the accumulation of PtdIns(3)P in the SARA-localized vesicular compartment. Our data indicate that the other PI3K including class II PI3K-C2β and class III Vps34 are involved in PtdIns(3)P accumulation in this compartment. Another point of interest is that partial reductions (25∼30%) of SARA association with the endosomes by depletion of either PI3K-C2β or Vps34 (Fig. 7*B*) did not inhibit Smad2/3 phosphorylation (Fig. 1*C*), which suggests that such partial reductions of the SARA association with the endosomes do not compromise Smad signaling.

We observed that PI3K-C2α depletion suppressed TGFβ-induced Smad2/3 signaling in several different vascular EC of human and mouse origins, but not vascular smooth muscle or epithelial cells (Figs. 1 and 2). In addition, Smad2/3 phosphorylation mediated by caALK5 in HEK293 cells was also PI3K-C2α-dependent (Fig. 8). Therefore, there appears to be some cell type specificity concerning the PI3K-C2α dependence. A few explanations for this may be possible. Another class II PI3K member, PI3K-C2β, possesses the similarities to PI3K-C2α, in the distribution of the expression, the structure, the clathrin binding capacity, and the substrate specificity (7). Functionally, PI3K-C2β is necessary for growth factor signaling (48) and cell migration with its lamellipodial distribution (49). Therefore, in vascular smooth muscle cells and epithelial cells, PI3K-C2β may be able to compensate for PI3K-C2α depletion. Alternatively, it might be possible that TGFβ-induced Smad2/3 signaling could be cell type-specific, because it was reported that the dependence of Smad2/3 signaling on endocytosis differed, depending on cell type (50).

In EC, TGFβ-induced activation of Smad2/3 signaling pathway is linked to the up-regulation of VEGF-A gene expression (39, 41). Consistent with the essential role of PI3K-C2α in TGFβ-induced Smad signaling activation, TGFβ stimulation of VEGF-A expression was completely and specifically dependent on PI3K-C2α (Fig. 9). Interestingly, TGFβ-induced endothelial cell migration and tube formation were both dependent on VEGFR2 (Fig. 10). It is reasonable to conceive that VEGF-A-stimulated cell migration and tube formation requires PI3K-C2α because VEGFR2 signaling and transport of VE-cadherin and other molecules are dependent on vesicular trafficking (8, 51). Hence, TGFβ-induced stimulation of these cellular responses requires PI3K-C2α for at least at two steps, *i.e.* TGFβ-induced Smad2/3 signaling-dependent VEGF expression and VEGF activation of VEGFR2 signaling. PI3K-C2α has a significant *in vivo* functional role in TGFβ-induced neovessel formation at an organismal level as demonstrated by the observations in EC-specific PI3K-C2α-deleted mice (Fig. 12).

Previous studies showed that TGFβ stimulated proliferation and migration of ECs via ALK1, whereas TGFβ inhibited proliferation and migration of ECs via ALK5 (24, 52), although some studies (41, 53) showed that ALK5-mediated stimulation of cell migra-

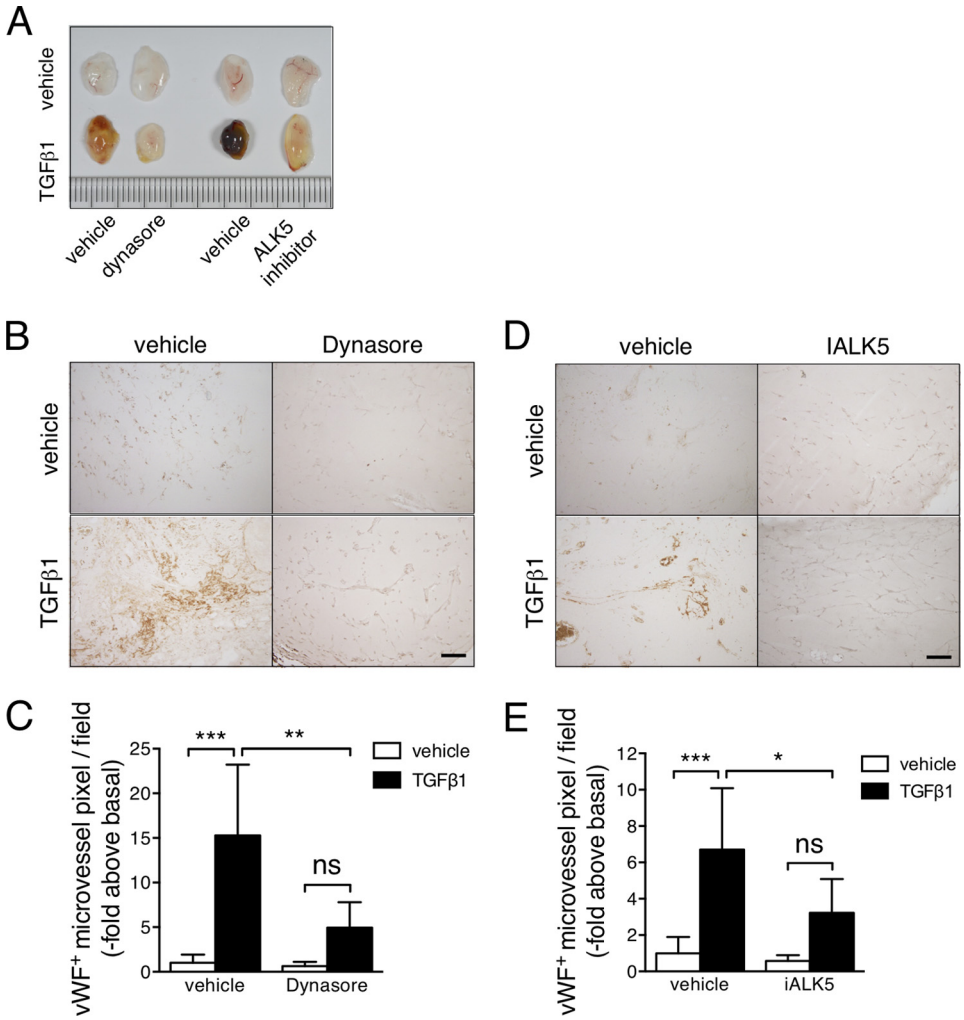

FIGURE 12. **Receptor endocytosis and ALK5 are necessary for TGFβ1-induced angiogenesis *in vivo*.** Matrigels containing of PBS (*vehicle*) or TGFβ1 and dynasore (200 μM) or iALK5 (20 μM) were injected into the subcutaneous tissues on the back. Matrigel plugs were removed 10 days later and analyzed for microvascular formation by immunohistochemistry using anti-vWF antibody. *A*, representative gross views of Matrigel plugs resected from mice. *B* and *D*, representative views of anti-vWF immunostained sections of Matrigel plugs containing dynasore (*left panel*) and iALK5 (*right panel*). *C* and *E*, quantified data of the effects of dynasore and iALK5 on neovessel formation in Matrigel plugs (six mice per group).

tion. The present observations suggest that ALK5-mediated stimulation of EC migration involves an indirect mechanism, *i.e.* stimulation by autocrine/paracrine VEGF. TGFβ-induced phosphorylation of Smad1/5/8 was dependent on PI3K-C2α, as well as Smad2/3 phosphorylation (Fig. 2*A*). It is intriguing to see how ALK1-mediated Smad1/5/8 phosphorylation is dependent on PI3K-C2α in a future study.

In summary, the present study indicates that PI3K-C2α is indispensable for TGFβ-induced Smad signaling through being engaged in the internalization of TGFβ receptors into the Smad anchor SARA-containing early endosomes. Thus, our study suggests that PI3K-C2α is essential for endosomal signaling of TGFβ receptors. The elucidation of the role for PI3K-C2α in TGFβ receptor signaling opens the new avenue for understanding in more depth normal TGFβ actions and their derangements in diseases.

REFERENCES

1. Engelman, J. A., Luo, J., and Cantley, L. C. (2006) The evolution of phosphatidylinositol 3-kinases as regulators of growth and metabolism. *Nat. Rev. Genet.* **7,** 606–619
2. Vanhaesebroeck, B., Guillermet-Guibert, J., Graupera, M., and Bilanges, B. (2010) The emerging mechanisms of isoform-specific PI3K signalling. *Nat. Rev. Mol. Cell Biol.* **11,** 329–341
3. Virbasius, J. V., Guilherme, A., and Czech, M. P. (1996) Mouse p170 is a novel phosphatidylinositol 3-kinase containing a C2 domain. *J. Biol. Chem.* 271, 13304–13307
4. Molz, L., Chen, Y. W., Hirano, M., and Williams, L. T. (1996) Cpk is a novel class of *Drosophila* PtdIns 3-kinase containing a C2 domain. *J. Biol. Chem.* **271,** 13892–13899
5. Domin, J., Pages, F., Volinia, S., Rittenhouse, S. E., Zvelebil, M. J., Stein, R. C., and Waterfield, M. D. (1997) Cloning of a human phosphoinositide 3-kinase with a C2 domain that displays reduced sensitivity to the inhibitor wortmannin. *Biochem. J.* **326,** 139–147
6. Traer, C. J., Foster, F. M., Abraham, S. M., and Fry, M. J. (2006) Are class II phosphoinositide 3-kinases potential targets for anticancer therapies? *Bull. Cancer* **93,** E53–E58
7. Falasca, M., and Maffucci, T. (2012) Regulation and cellular functions of class II phosphoinositide 3-kinases. *Biochem. J.* **443,** 587–601
8. Yoshioka, K., Yoshida, K., Cui, H., Wakayama, T., Takuwa, N., Okamoto, Y., Du, W., Qi, X., Asanuma, K., Sugihara, K., Aki, S., Miyazawa, H., Biswas, K., Nagakura, C., Ueno, M., Iseki, S., Schwartz, R. J., Okamoto, H., Sasaki, T., Matsui, O., Asano, M., Adams, R. H., Takakura, N., and Takuwa, Y. (2012) Endothelial PI3K-C2α, a class II PI3K, has an essential role in an-

giogenesis and vascular function. *Nat. Med.* **18,** 1560–1569
9. Domin, J., Gaidarov, I., Smith, M. E., Keen, J. H., and Waterfield, M. D. (2000) The class II phosphoinositide 3-kinase PI3K-C2α is concentrated in the trans-Golgi network and present in clathrin-coated vesicles. *J. Biol. Chem.* **275,** 11943–11950
10. Gaidarov, I., Smith, M. E., Domin, J., and Keen, J. H. (2001) The class II phosphoinositide 3-kinase C2α is activated by clathrin and regulates clathrin-mediated membrane trafficking, *Mol. Cell* **7,** 443–449
11. Borner, G. H., Antrobus, R., Hirst, J., Bhumbra, G. S., Kozik, P., Jackson, L. P., Sahlender, D. A., and Robinson, M. S. (2012) Multivariate proteomic profiling identifies novel accessory proteins of coated vesicles. *J. Cell Biol.* **197,** 141–160
12. Falasca, M., Hughes, W. E., Dominguez, V., Sala, G., Fostira, F., Fang, M. Q., Cazzolli, R., Shepherd, P. R., James, D. E., and Maffucci, T. (2007) The role of phosphoinositide 3-kinase C2α in insulin signaling. *J. Biol. Chem.* **282,** 28226–28236
13. Leibiger, B., Moede, T., Uhles, S., Barker, C. J., Creveaux, M., Domin, J., Berggren, P. O., and Leibiger, I. B. (2010) Insulin-feedback via PI3K-C2α activated PKBα/Akt1 is required for glucose-stimulated insulin secretion. *FASEB J.* **24,** 1824–1837
14. Posor, Y., Eichhorn-Gruenig, M., Puchkov, D., Schöneberg, J., Ullrich, A., Lampe, A., Müller, R., Zarbakhsh, S., Gulluni, F., Hirsch, E., Krauss, M., Schultz, C., Schmoranzer, J., Noé, F., and Haucke, V. (2013) Spatiotemporal control of endocytosis by phosphatidylinositol-3,4-bisphosphate. *Nature* **499,** 233–237
15. Biswas, K., Yoshioka, K., Asanuma, K., Okamoto, Y., Takuwa, N., Sasaki, T., and Takuwa, Y. (2013) Essential role of class II phosphatidylinositol-3-kinase-C2α in sphingosine 1-phosphate receptor-1-mediated signaling and migration in endothelial cells. *J. Biol. Chem.* **288,** 2325–2339
16. Biswas, K., Yoshioka, K., Aki, S., Cui, H., Zhao, J., Kuda, Y., Takuwa, N., Okamoto, Y., and Takuwa, Y. (2013) Class II PI3K-C2α plays essential role in endosomal Rac1 activation and cell migration in S1P-stimulated endothelial cells. *J. Physiol. Sci.* **63,** S136
17. Oshima, M., Oshima, H., and Taketo, M. M. (1996) TGF-β receptor type II deficiency results in defects of yolk sac hematopoiesis and vasculogenesis. *Dev. Biol.* **179,** 297–302
18. Larsson, J., Goumans, M. J., Sjöstrand, L. J., van Rooijen, M. A., Ward, D., Levéen, P., Xu, X., ten Dijke, P., Mummery, C. L., and Karlsson, S. (2001) Abnormal angiogenesis but intact hematopoietic potential in TGF-β type I receptor-deficient mice. *EMBO J.* **20,** 1663–1673
19. Carvalho, R. L., Jonker, L., Goumans, M. J., Larsson, J., Bouwman, P., Karlsson, S., Dijke, P. T., Arthur, H. M., and Mummery, C. L. (2004) Defective paracrine signalling by TGFβ in yolk sac vasculature of endoglin mutant mice: a paradigm for hereditary haemorrhagic telangiectasia. *Development* **131,** 6237–6247
20. Carvalho, R. L., Itoh, F., Goumans, M. J., Lebrin, F., Kato, M., Takahashi, S., Ema, M., Itoh, S., van Rooijen, M., Bertolino, P., ten Dijke, P., and Mummery, C. L. (2007) Compensatory signalling induced in the yolk sac vasculature by deletion of TGFβ receptors in mice. *J. Cell Sci.* **120,** 4269–4277
21. Heldin, C. H., Miyazono, K., and ten Dijke, P. (1997) TGF-β signalling from cell membrane to nucleus through SMAD proteins. *Nature* **390,** 465-471
22. ten Dijke, P., and Arthur, H. M. (2007) Extracellular control of TGFβ signalling in vascular development and disease. *Nat. Rev. Mol. Cell Biol.* **8,** 857–869
23. Pardali, E., Goumans, M. J., and ten Dijke, P. (2010) Signaling by members of the TGF-β family in vascular morphogenesis and disease. *Trends Cell Biol.* **20,** 556–567
24. Goumans, M. J., Valdimarsdottir, G., Itoh, S., Lebrin, F., Larsson, J., Mummery, C., Karlsson, S., ten Dijke, P. (2003) Activin receptor-like kinase (ALK)1 is an antagonistic mediator of lateral TGFβ/ALK5 signaling. *Mol. Cell* **12,** 817–828
25. Pardali, E., and ten Dijke, P. (2012) TGFβ signaling and cardiovascular diseases. *Int. J. Biol. Sci.* **8,** 195–213
26. Itoh, F., Itoh, S., Adachi, T., Ichikawa, K., Matsumura, Y., Takagi, T., Festing, M., Watanabe, T., Weinstein, M., Karlsson, S., and Kato, M. (2012) Smad2/Smad3 in endothelium is indispensable for vascular stability via S1PR1 and N-cadherin expressions. *Blood* **119,** 5320–5328
27. Lan, Y., Liu, B., Yao, H., Li, F., Weng, T., Yang, G., Li, W., Cheng, X., Mao, N., and Yang, X. (2007) Essential role of endothelial Smad4 in vascular remodeling and integrity. *Mol. Cell. Biol.* **27,** 7683–7692
28. Tsukazaki, T., Chiang, T. A., Davison, A. F., Attisano, L., and Wrana, J. L. (1998) SARA, a FYVE domain protein that recruits Smad2 to the TGFβ receptor. *Cell* **95,** 779–791
29. Itoh, F., Divecha, N., Brocks, L., Oomen, L., Janssen, H., Calafat, J., Itoh, S., and ten Dijke, P. (2002) The FYVE domain in Smad anchor for receptor activation (SARA) is sufficient for localization of SARA in early endosomes and regulates TGF-β/Smad signaling. *Genes Cells* **7,** 321–331
30. Hayes, S., Chawla, A., and Corvera, S. (2002) TGF β receptor internalization into EEA1-enriched early endosomes: role in signaling to Smad2. *J. Cell Biol.* **158,** 1239–1249
31. Di Guglielmo, G. M., Le Roy, C., Goodfellow, A. F., and Wrana, J. L. (2003) Distinct endocytic pathways regulate TGF-β receptor signalling and turnover. *Nat Cell Biol.* **5,** 410–421
32. Du, W., Takuwa, N., Yoshioka, K., Okamoto, Y., Gonda, K., Sugihara, K., Fukamizu, A., Asano, M., and Takuwa, Y. (2010) S1P2, the G protein-coupled receptor for sphingosine-1-phosphate,negatively regulates tumor angiogenesis and tumor growth *in vivo* in mice. *Cancer Res.* **70,** 772–781
33. Cui, H., Okamoto, Y., Yoshioka, K., Du, W., Takuwa, N., Zhang, W., Asano, M., Shibamoto, T., and Takuwa, Y. (2013) Sphingosine-1-phosphate receptor-2 protects against anaphylactic shock through suppression of eNOS in mice. *J. Allergy Clin. Immunol.* **132,** 1205–1214
34. Okamoto, H., Takuwa, N., Yokomizo, T., Sugimoto, N., Sakurada, S., Shigematsu, H., and Takuwa, Y. (2000) Inhibitory regulation of Rac activation, membrane ruffling and cell migration by sphingosine-1-phosphate receptor EDG5, but not EDG1 or EDG3. *Mol. Cell. Biol.* **20,** 9247–9261
35. Mizuide, M., Hara, T., Furuya, T., Takeda, M., Kusanagi, K., Inada, Y., Mori, M., Imamura, T., Miyazawa, K., and Miyazono, K. (2003) Two short segments of Smad3 are important for specific interaction of Smad3 with c-Ski and SnoN. *J. Biol. Chem.* **278,** 531–536
36. Inoki, I., Takuwa, N., Sugimoto, N., Yoshioka, K., Takata, S., Kaneko, S., and Takuwa, Y. (2006) Negative regulation of endothelial morphogenesis and angiogenesis by S1P2 receptor. *Biochem. Biophys. Res. Commun.* **346,** 293–300
37. Guo, X., and Wang, X. F. (2009) Signaling cross-talk between TGF-β/BMP and other pathways. *Cell Res.* **19,** 71–88
38. Breier, G., Blum, S., Peli, J., Groot, M., Wild, C., Risau, W., and Reichmann, E. (2002) Transforming growth factor-β and Ras regulate the VEGF/VEGF-receptor system during tumor angiogenesis. *Int. J. Cancer.* **97,** 142–148
39. Boström, K., Zebboudj, A. F., Yao, Y., Lin, T. S., and Torres, A. (2004) Matrix GLA protein stimulates VEGF expression through increased transforming growth factor-β1 activity in endothelial cells. *J. Biol. Chem.* **279,** 52904–52913
40. Clifford, R. L., Deacon, K., and Knox, A. J. (2008) Novel regulation of vascular endothelial growth factor-A (VEGF-A) by TGFβ1: requirement for Smads, β-catenin and GSK3β. *J. Biol. Chem.* **283,** 35337–35353
41. Shao, E. S., Lin, L., Yao, Y., and Boström, K. I. (2009) Expression of vascular endothelial growth factor is coordinately regulated by the activin-like kinase receptors 1 and 5 in endothelial cells. *Blood* **114,** 2197–2206
42. Bakkebø, M., Huse, K., Hilden, V. I., Forfang, L., Myklebust, J. H., Smeland, E. B., Oksvold, M. P. (2012) SARA is dispensable for functional TGF-β signaling. *FEBS Lett.* **586,** 3367–3372
43. Lu, Z., Murray, J. T., Luo, W., Li, H., Wu, X., Xu, H., Backer, J. M., Chen, Y. G. (2002) Transforming growth factor β activates Smad2 in the absence of receptor endocytosis. *J. Biol. Chem.* **277,** 29363–29368
44. Scita, G., and Di Fiore, P. P. (2010) The endocytic matrix. *Nature* **463,** 464–473
45. Panopoulou, E., Gillooly, D. J., Wrana, J. L., Zerial, M., Stenmark, H., Murphy, C., and Fotsis, T. (2002) Early endosomal regulation of Smad-dependent signaling in endothelial cells. *J. Biol. Chem.* **277,** 18046–18052
46. Maffucci, T., Brancaccio, A., Piccolo, E., Stein, R. C., and Falasca, M. (2003) Insulin induces phosphatidylinositol-3-phosphate formation through TC10 activation. *EMBO J.* **22,** 4178–4189

47. Wang, Y., Yoshioka, K., Azam, M. A., Takuwa, N., Sakurada, S., Kayaba, Y., Sugimoto, N., Inoki, I., Kimura, T., Kuwaki, T., and Takuwa, Y. (2006) Class II phosphoinositide 3-kinase alfa-isoform regulates Rho, myosin phosphatase and contraction in vascular smooth muscle. *Biochem. J.* **394,** 581–592
48. Harada, K., Truong, A. B., Cai, T., and Khavari, P. A. (2005) The class II phosphoinositide 3-kinase C2β is not essential for epidermal differentiation. *Mol. Cell. Biol.* **25,** 11122–11130
49. Maffucci, T., Cooke, F. T., Foster, F. M., Traer, C. J., Fry, M. J., and Falasca, M. (2005) Class II phosphoinositide 3-kinase defines a novel signaling pathway in cell migration. *J. Cell Biol.* **169,** 789–799
50. Runyan, C. E., Schnaper, H. W., and Poncelet, A. C. (2005) The role of internalization in transforming growth factor β1-induced Smad2 association with Smad anchor for receptor activation (SARA) and Smad2-dependent signaling in human mesangial cells. *J. Biol. Chem.* **280,** 8300–8308
51. Simons, M. (2012) An inside view: VEGF receptor trafficking and signaling. *Physiol.* (*Bethesda*) **27,** 213–222
52. Goumans, M. J., Valdimarsdottir, G., Itoh, S., Rosendahl, A., Sideras, P., ten Dijke, P. (2002) Balancing the activation state of the endothelium via two distinct TGF-β type I receptors. *EMBO J.* 21, 1743–1753
53. Lamouille, S., Mallet, C., Feige, J. J., Bailly, S. (2002) Activin receptor-like kinase 1 is implicated in the maturation phase of angiogenesis. *Blood* **100,** 4495–4501